of 261 (7%, 95% CI 4·1–10·7) and six of 149 children (4%, 1·7–8·2), respectively. We isolated the last poliovirus from a stool sample collected 1 month after the OPV/IPV switch. We did not detect any polioviruses in 223 stool samples collected during the post-transitional period. The Cochram-Armitage test shows a significant trend ($p<0·0001$) in prevalence across the three periods. We recorded the demographic features of the 24 poliovirus-positive and 609 poliovirus-negative children (webappendix 1). All polioviruses were isolated from vaccinees who had OPV within 10 weeks of being admitted to hospital and who were younger than age 6 months. Poliovirus isolation rates were similar across all socioeconomic groups. 24 inpatients yielded 30 Sabin-like polioviruses (seven type 1, 12 type 2, 11 type 3).

Since 1997 there has been continued monitoring of acute flaccid paralysis in children younger than age 15 years.[4] Between January, 2001, and September, 2003, we analysed stool samples from 22 of 33 reported cases of acute flaccid paralysis. Only one child, aged 2 months and with spinal muscular atrophy, had Sabin-like polioviruses type 1 and type 2 isolated from each of two stool samples collected on Feb 28 and March 1, 2001. She had received her first dose of OPV 11 days previously.

Enterovirus surveillance used the national laboratory network, which investigates mainly inpatients with febrile illnesses not associated with acute flaccid paralysis (about 1200 stool samples annually).[5] We analysed data for 33 months (13 months before, 2 months during, and 18 months after the switch) and noted that polioviruses disappeared rapidly after the OPV/IPV switch (webappendix 2). Before the switch, we identified 38 poliovirus-positive children. In the transition period, we isolated Sabin-like polioviruses type 1 and type 2 from a 2-month-old boy without acute flaccid paralysis, whose stool sample was collected 5 days after the OPV/IPV switch. 19 months later, we identified a Sabin-like poliovirus type 2 in a 10-month-old girl with conjunctivitis. Sequencing in the VP1 region showed 99·9% homology to the parental Sabin strain. Almost all poliovirus-positive cases from enterovirus surveillance were aged 6 weeks to 5 months. 40 children without acute flaccid paralysis yielded 48 Sabin-like polioviruses (19 type 1, 18 type 2, 11 type 3).

For environmental surveillance, we collected weekly sewage samples over 18 months (3 months before, 2 months during, and 13 months after the switch) from three sewage treatment plants in Auckland, Hamilton, and Porirua (a satellite city of Wellington) where the surveillance hospitals were located. The catchment populations were 900 000, 100 000, and 65 000, respectively. Before the OPV/IPV switch, the poliovirus isolation rate was 94%. This proportion decreased after the switch, but not as rapidly as with other surveillance methods (figure 2). The decline was maintained in the post-transitional period (April, 2002, to April, 2003), such that after May, 2002, polioviruses were only detected once every 3 months.

We isolated 71 Sabin-like polioviruses as a result of environmental surveillance (nine type 1, 36 type 2, 26 type 3). Sequencing of environmental polioviruses during the post-transitional period confirmed these as Sabin-like with more than 99% homology with parental Sabin strains (webappendix 3). In particular, the five Sabin-like polioviruses identified by environmental

and Enterovirus Section, National Center for Infectious Diseases, Centers for Disease Control and Prevention, Atlanta, Georgia, USA (M A Pallansch PhD)

Correspondence to:
Dr Q Sue Huang
Sue.Huang@esr.cri.nz

See Lancet Online for webappendix 1

See Lancet Online for webappendix 2 and webappendix 3

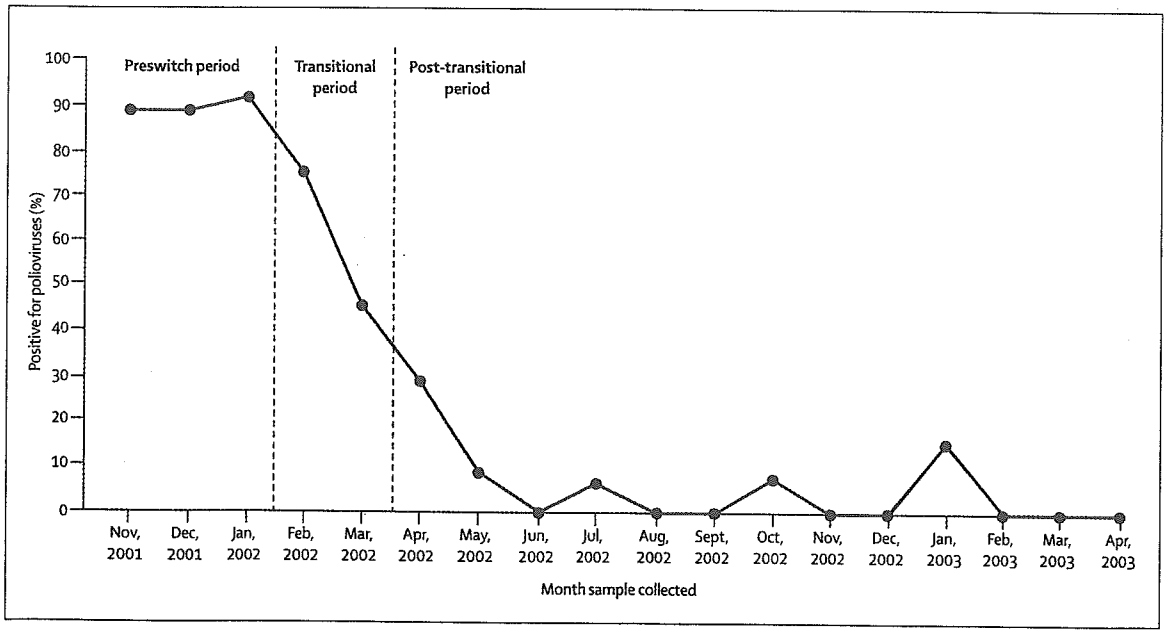


*Figure 2:* **Poliovirus prevalence between November, 2001, and April, 2003, by environmental surveillance**

surveillance 6, 9, and 12 months after the OPV/IPV switch had 99·7–100% homology with parental strains.

We noted limited circulation of OPV strains in New Zealand after the switch to IPV. First, with one exception, all polioviruses isolated from enterovirus surveillance during 2001–02 were from children aged 6 weeks to 5 months who should have received at least one dose of OPV. Second, OPV viruses detected by paediatric-inpatient surveillance were found only in vaccinees. Third, intratypic differentiation and sequence data for polioviruses obtained from paediatric-inpatient, acute flaccid paralysis, and enterovirus surveillance confirmed that all polioviruses were Sabin-like.

Since polioviruses evolve at a constant rate of 1% nucleotide substitutions per year,[6] environmental isolates 6–12-months post-switch with 99·7–100% sequence homology to parental Sabin strains infer that these viruses were derived from OPV administered 1–3-months previously. Rather than being from either the last cohorts of OPV immunised children or immune-deficient long-term excretors,[7] these viruses are more likely to have originated in recently vaccinated children or their close contacts from an OPV-using country. This finding shows that New Zealand remains vulnerable to vaccine or wildtype virus importation.

Every surveillance method revealed a different rate of OPV virus decline. Acute flaccid paralysis surveillance examines as few as 1 in 100 000 children younger than 15 years for poliovirus excretion. Its sensitivity for detecting sporadic vaccine-derived poliovirus is limited since only 0·1–0·5% of non-immune children infected with virulent strains will manifest paralytic poliomyelitis. Every year, enterovirus surveillance examines stool samples from roughly one in 3000 (1200 of 3 737 277) New Zealanders suspected of enteroviral infections. Paediatric-inpatient surveillance attempted to measure poliovirus excretion in a moderately representative population by sampling one in 648 (633 of 410 181) children living in three cities. Environmental surveillance obtained composite samples from sewage systems that serve 28% of the population. The higher and more prolonged poliovirus detection rates in sewage indicate the increased sensitivity of this method of surveillance over that of paediatric-inpatient surveillance in the same urban areas.

OPV strains do not persist for long after an OPV/IPV switch in a developed country with a temperate climate. Our study should be repeated in tropical, developing countries, however, where transmission of OPV viruses is likely to be more intense. The findings of such studies are vital to formulate polio immunisation policies in the postcertification era. Simultaneous global cessation of OPV after a mass immunisation campaign to maximise population immunity and minimise vaccine-derived poliovirus circulation could be adopted if there is minimum risk of sustained vaccine-derived poliovirus circulation.[2] Meanwhile, the continued risk of poliovirus importation means that New Zealand should maintain high IPV coverage. Finally, multiple surveillance methods, particularly environmental surveys, provide increased sensitivity for detection of poliovirus circulation, which will be essential in the posteradication era.

**Contributors**

Q S Huang, G Greening, M G Baker, and K Grimwood designed the study, supervised the virological, clinical, and environmental components, interpreted the data and their analysis, and wrote the report. J Hewitt, D Hulston, L van Duin, and A Fitzsimons established and did the laboratory tests. N Garrett did the study size calculations, contributed to the design, and undertook statistical analyses. K Grimwood, D Graham, and D Lennon established paediatric-inpatient surveillance. H Shimizu and T Miyamura undertook the sequence analysis and interpretation. M A Pallansch assisted in study design and interpretation.

**Conflict of interest statement**

We declare that we have no conflict of interest.

**Acknowledgments**

We thank David Wood, David Featherstone, and Walter Dowdle for their helpful advice; Elizabeth Sneyd and Ruth Pirie for help with data analysis; Andi Utama for sequence analysis; the paediatric nurses at Middlemore, Waikato, and Wellington Hospitals for stool and questionnaire collection; staff at the Porirua, Hamilton, and Mangere sewage treatment plants for sewage collection; and staff at the Institute of Environmental Science and Research who provided logistic, administrative, and technical support.

The study was supported by a grant (B3/181/124) from the Department of Vaccines and Biologicals, WHO. Surveillance of enterovirus and acute flaccid paralysis received financial support from the New Zealand Ministry of Health who permitted publication of the relevant data. The sponsors of the study had no role in study design, data collection, data analysis, data interpretation, or writing of the report. The corresponding author had full access to all the data in the study and had final responsibility for the decision to submit for publication.

**References**

1 Wood DJ, Sutter RW, Dowdle WR. Stopping poliovirus vaccination after eradication: issues and challenges. *Bull World Health Organ* 2000; 78: 347–57.

2 Dowdle WR, De Gourville E, Kew OM, Pallansch MA, Wood DJ. Polio eradication: the OPV paradox. *Rev Med Virol* 2003; 13: 277–91.

3 Mas Lago P. Eradication of poliomyelitis in Cuba: a historical perspective. *Bull World Health Organ* 1999; 77: 681–87.

4 Heffernan H, Edwards E, Grant C, Huang QS. A case of vaccine-associated paralytic poliomyelitis. *New Zealand Public Health Report* 1999; 6: 33–35.

5 Huang QS, Carr JM, Nix WA, et al. An echovirus type 33 winter outbreak in New Zealand. *Clin Infect Dis* 2003; 37: 650–57.

6 Yang CF, Naguib T, Yang SJ, et al. Circulation of endemic type 2 vaccine-derived poliovirus in Egypt from 1983 to 1993. *J Virol* 2003; 77: 8366–77.

7 Halsey NA, Pinto J, Espinosa-Rosales F, et al. Search for poliovirus carriers among people with primary immune deficiency diseases in the United States, Mexico, Brazil, and the United Kingdom. *Bull World Health Organ* 2004; 82: 3–8.

Reprints Coordinator
John Fyfe
T: +44 (0)20 7424 4329
F: +44 (0)20 7424 4286
john.fyfe@lancet.com

*The Lancet* is a weekly subscription journal. For further information on how to subscribe please contact our Subscription Department
T: +44 (0) 1865 843077
F: +44 (0) 1865 843970
custserv@lancet.com

(North America)
T: +1 (800) 462 6198
F: +1 (800) 327 9021
USLancetCS@elsevier.com

Printed in UK by Lynhurst Press Ltd

*Journal of General Virology* (2005), **86**, 1391–1401 DOI 10.1099/vir.0.80784-0

# Temperature-sensitive mutants of enterovirus 71 show attenuation in cynomolgus monkeys

Minetaro Arita,[1] Hiroyuki Shimizu,[1] Noriyo Nagata,[2] Yasushi Ami,[3] Yuriko Suzaki,[3] Tetsutaro Sata,[2] Takuya Iwasaki[4] and Tatsuo Miyamura[1]

Correspondence
Minetaro Arita
minetaro@nih.go.jp

[1,2,3]Department of Virology II[1], Department of Pathology[2] and Division of Experimental Animals Research[3], National Institute of Infectious Diseases, 4-7-1 Gakuen, Musashimurayama-shi, Tokyo 208-0011, Japan

[4]Division of Clinical Investigation, Institute of Tropical Medicine, Nagasaki University, Nagasaki 852-8523, Japan

Enterovirus 71 (EV71) is one of the major causative agents of hand, foot and mouth disease and is sometimes associated with serious neurological disorders. In this study, an attempt was made to identify molecular determinants of EV71 attenuation of neurovirulence in a monkey infection model. An infectious cDNA clone of the virulent strain of EV71 prototype BrCr was constructed; temperature-sensitive (*ts*) mutations of an attenuated strain of EV71 or of poliovirus (PV) Sabin vaccine strains were then introduced into the infectious clone. *In vitro* and *in vivo* phenotypes of the parental and mutant viruses were analysed in cultured cells and in cynomolgus monkeys, respectively. Mutations in 3D polymerase ($3D^{pol}$) and in the 3′ non-translated region (NTR), corresponding to *ts* determinants of Sabin 1, conferred distinct temperature sensitivity to EV71. An EV71 mutant [EV71(S1-3′)] carrying mutations in the 5′ NTR, $3D^{pol}$ and in the 3′ NTR showed attenuated neurovirulence, resulting in limited spread of virus in the central nervous system of monkeys. These results indicate that EV71 and PV1 share common genetic determinants of neurovirulence in monkeys, despite the distinct properties in their original pathogenesis.

Received 25 November 2004
Accepted 3 February 2005

## INTRODUCTION

Enterovirus 71 (EV71) belongs to the genus *Enterovirus* of the family *Picornaviridae* and possesses a single-stranded, positive-sense RNA genome of approximately 7500 nt in length (Brown & Pallansch, 1995; Schmidt *et al.*, 1974). Genetically, EV71 is classified as a species A human enterovirus along with some coxsackie A (CA) viruses, such as CA10 and CA16 (Brown & Pallansch, 1995; Pulli *et al.*, 1995). As well as CA10 and CA16, EV71 causes hand, foot and mouth disease (HFMD) and herpangina, which are common and self-limiting diseases that typically occur in children. However, EV71 infection sometimes causes severe neurological diseases, such as brainstem encephalitis and polio-like paralysis (Chumakov *et al.*, 1979; Wang *et al.*, 2003), mainly in infants and young children (McMinn, 2002). A number of fatal encephalitis cases were reported in large-scale HFMD outbreaks in Malaysia in 1997 (Abubakar *et al.*, 1999; Shimizu *et al.*, 1999) and in Taiwan in 1998 and 2000 (Ho *et al.*, 1999; Lin *et al.*, 2003; Lu *et al.*, 2002; Wang *et al.*, 2002). Furthermore, sporadic HFMD cases with severe neurological manifestations have been reported in the Western Pacific region, e.g. in Australia, Singapore, Hong Kong and Japan (Ahmad, 2000; Chan *et al.*, 2000; Fujimoto *et al.*, 2002; Herrero *et al.*, 2003; Komatsu *et al.*, 1999; Lum *et al.*, 1998; McMinn *et al.*, 1999, 2001b). Numerous factors (e.g. virus genotypes or specific mutations, herd protective immunity, individual immunity or association with other infectious agents) could lead HFMD to become a more serious disease. From molecular epidemiological studies of EV71, McMinn *et al.* (2001a) suggested that an amino acid change at position 170 of VP1 (from Ala to Val) is involved in the virulence of EV71. Non-structural proteins of EV71 (2A and 3C proteinases) were responsible for the induction of apoptosis in infected cells *in vitro* (Kuo *et al.*, 2002; Li *et al.*, 2002). However, crucial epidemiological or experimental evidence to identify critical factors of EV71 pathogenesis has yet to be provided (Shimizu *et al.*, 1999).

The occasional association of EV71 infection with serious neurological manifestations suggests that EV71 is highly neurotropic, like poliovirus (PV), which is the causative agent of poliomyelitis. The molecular determinants of the neurovirulence of PV have been studied extensively on the vaccine strains (Sabin 1, 2 and 3) (reviewed by Minor, 1992) in monkeys, as well as in transgenic mice carrying the

The GenBank/EMBL/DDBJ accession numbers for the complete genomic sequences of EV71(BrCr-TR) and EV71(BrCr-ts) are AB204852 and AB204853, respectively.

human PV receptor gene (Horie *et al.*, 1994; Koike *et al.*, 1993; Ren *et al.*, 1990). In contrast, the molecular basis of EV71 neuropathogenicity remains poorly understood, partly due to the lack of appropriate infection models.

Recently, we established an experimental EV71 infection of cynomolgus monkeys by using intravenous inoculation (Nagata *et al.*, 2004). This new experimental system of EV71 consistently induced typical neurological manifestations similar to those observed in human cases, including tremor, ataxia and polio-like paralysis (Nagata *et al.*, 2004). These disorders were caused by encephalomyelitis, involving both the pyramidal and extrapyramidal systems, in monkeys. These neurological manifestations were difficult to assess in current mouse models, where some clinical symptoms, including rash and hind-limb paralysis, were observed and adaptive mutations of EV71 played a critical role in the virulence (Chen *et al.*, 2004; Wang *et al.*, 2004). Not all of the EV71 isolates, irrespective of their clinical backgrounds, could achieve infection in mice (N. Nagata, H. Shimizu & T. Iwasaki, unpublished data). Therefore, we applied a monkey infection model for the evaluation of genetic determinants of EV71 neurovirulence.

In this study, we established an infectious cDNA clone derived from the prototype BrCr strain of EV71 and examined the effect of temperature-sensitive (*ts*) mutations on neurovirulence in a monkey infection model. We analysed a *ts* variant of the BrCr strain [EV71(BrCr-ts)] with an attenuated phenotype (Hagiwara *et al.*, 1983; Hashimoto & Hagiwara, 1983) to identify the critical mutations for its *ts* phenotype. We examined the effect of *ts* determinants of Sabin strains in the context of the EV71(BrCr) genome on the attenuation.

## METHODS

**Cells and viruses.** Vero cells (derived from African green monkey kidney cells) were maintained in Dulbecco's modified Eagle's medium (DMEM) supplemented with 5% fetal calf serum (FCS) and were used for virus preparation, titration and measurement of growth kinetics and temperature sensitivity. *ts* and temperature-resistant (*tr*) variants of the prototype BrCr strain (Schmidt *et al.*, 1974), EV71(BrCr-ts) and EV71(BrCr-TR), were isolated previously in cynomolgus monkey kidney (CMK) cells (Hagiwara *et al.*, 1983; Hashimoto & Hagiwara, 1983). EV71(BrCr-ts) showed an attenuated phenotype and EV71(BrCr-TR) retained the neurovirulent phenotype of the BrCr strain in cynomolgus monkeys (Hashimoto & Hagiwara, 1983; Nagata *et al.*, 2002, 2004). The variants used in this study were obtained after further plaque purification in Vero cells from the original virus stock. The viral genomes of plaque-purified variants had mutations compared with the parental BrCr strain. The virus stocks were prepared in Vero cells by RNA transfection of the transcripts derived from corresponding infectious clones.

**RNA extraction, RT-PCR and sequencing.** Viral genomic RNA was extracted from the culture fluid of infected cells by using a High Pure viral RNA purification kit (Roche). RT-PCR was performed by using RevatraAce reverse transcriptase (Toyobo) for reverse transcription and either Advantage 2 polymerase (Clontech) or *Tbr* EXT DNA polymerase (Finnzymes) for PCR. PCR products were purified by using a PCR purification kit (Qiagen). Direct sequence analysis was carried out on the full-length genomic sequences of EV71(BrCr-TR) or EV71(BrCr-ts), using DNA fragments amplified by RT-PCR as the templates of the sequence reaction. The sequence of the 5′ end of the viral genome was determined by using a 5′ RACE (rapid amplification of cDNA ends) system, ver. 2.0 (Invitrogen), according to the manufacturer's instructions. The sequence of the 3′ end of the viral genomes was determined from an RT-PCR product obtained with primers 7200F+ and *Eco*RI-3END− (Table 1). DNA sequencing was performed by using a BigDye Terminator v3.0 cycle sequencing ready reaction kit (Applied Biosystems) and then analysed by an ABI PRISM 310 genetic analyser (Applied Biosystems).

**General methods of molecular cloning.** Two *Escherichia coli* strains were used for the preparation of plasmids. The TOP10 strain (Invitrogen) was used for direct cloning of PCR products, using a TOPO XL PCR cloning kit (Invitrogen). The XL10gold strain (Stratagene) was used for the preparation of other plasmids. Ligation of DNA fragments was performed by using a Quick Ligation kit (New England Biolabs). Site-directed mutagenesis was performed by using KOD plus DNA polymerase (Toyobo) (Sambrook & Russell, 2001).

**Construction of the infectious cDNA clone of EV71(BrCr-TR).** A DNA fragment containing 6 kb of the 3′ region of the viral genome was amplified by RT-PCR using Advantage 2 polymerase (Clontech) from the viral genome of EV71(BrCr-TR) with primers EV71-1500F+ and EV71-A2− (Table 1). The resultant cDNA fragment was cloned into plasmid pCR-XL-TOPO by using a TOPO XL PCR cloning kit (Invitrogen). Next, the 5′ end sequence of EV71(BrCr-TR) was amplified by RT-PCR with primers *Pvu*T7-45+ and 1595R− and then cloned into the above construct following digestion by *Pvu*I and *Mun*I. However, the RNA transcript derived from the resultant full-length cDNA of EV71(BrCr-TR) did not produce any viable viruses after RNA transfection into Vero cells (data not shown). Therefore, to remove possible lethal mutation(s) in the construct, the 3′ part of the cDNA fragment of EV71(BrCr-TR) was obtained by RT-PCR using *Tbr* EXT DNA polymerase (Finnzymes) with primers A2*Bam*HI− and EV71-1500F+ (Table 1) and then cloned into the *Bam*HI site of the above construct. Transfection of the RNA transcript derived from this cDNA clone produced viable viruses in Vero cells. This infectious clone of EV71(BrCr-TR) was digested with *Sna*BI and *Mlu*I, and then cloned into plasmid P/H d40 (a generous gift from Dr E. Wimmer) (Zhao *et al.*, 2000). In this construct, to introduce *Mlu*I and *Sna*BI sites, part of the plasmid vector was obtained by PCR using *Tbr* EXT DNA polymerase (Finnzymes) with primers *Mlu*I-vec+ and *Sna*BI-vec−, using plasmid P/H d40 as the template DNA. There were five nucleotide differences between the sequence of the EV71(BrCr-TR) genome and that of the resultant infectious clone. To restore the sequence of the clone to the consensus sequence of the EV71(BrCr-TR) genome, the 5′ fragment was amplified again by RT-PCR with primers *Sna*BI-T7-EV71+ and 1595R−, using the viral genome of EV71(BrCr-TR) as the template. The obtained fragment was digested with *Mun*I and *Sna*BI and then ligated into the infectious clone. To restore other mutated sites, DNA fragments obtained with primers EV71-1500F+ and 71/3393−, with primers EV71-2800F+ and tr-6300R− or with primers E2 CF2+ and tr-6300R− were digested with *Mun*I and *Xma*I, with *Xma*I and *Sal*I or with *Sal*I and *Spe*I, respectively, and then ligated sequentially into the infectious clone. Finally, the resultant infectious clone was sequenced and confirmed to have the consensus sequence of the EV71(BrCr-TR) genome. This infectious clone of EV71(BrCr-TR) was designated pEV71(BrCr-TR).

**Construction of *ts* mutants.** We constructed *ts* mutants of EV71 by introducing the mutations of a *ts* variant of the BrCr strain [EV71(BrCr-ts)] (Hagiwara *et al.*, 1983; Hashimoto & Hagiwara, 1983) (Fig. 1). For the construction of a cDNA clone of EV71(ts-TR), a cDNA sequence was amplified from the EV71(BrCr-ts) genome by

**Table 1.** Primers used for the construction of the infectious clone of EV71(BrCr-TR)

| Primer name | Sequence (5′–3′) |
|---|---|
| 1595R− | TCCAGCGGGCTGATAGGCACCACC |
| 2784+ | CATAACCGGTCATGCGCAGATG |
| 2784− | CATCTGCGCATGACCGGTTATG |
| 3564− | CTCACTAGCTTCTACAAACACCAAACTAGG |
| 6153C+ | GAACCTGATGAGCACGTGACACAGGC |
| 6153C− | GCCTGTGTCACGTGCTCATCAGGTTC |
| 7023AT+ | GATAAATCACCTATTTTCAATGAGGTTAC |
| 7023AT− | GTAACCTCATTGAAAATAGGTGATTTATC |
| 7200F+ | AACACTCAAGATCACGTGCGCTCCC |
| 71/3393− | GGCGGTTRACCACYCTDAAGTTGCCCAC |
| 7409G− | AAAAACGCGTTTTTTTTTTTTTTTTTTTTTTTTTTTCGCTATTCTGGTTATAAC |
| A2*Bam*HI− | AAAAGGATCCTTTTTTTTTTTTTTTTTTTTTTTTTTGCTATTCTGG |
| E2 CF2+ | GAGCAAACACCGTATTGAACCTGTATG |
| *Eco*RI-3END− | ACTGGAATTCTTTTTTTTTTTTTTTTTTTTTTTTTV |
| EV71-1500F+ | GGATTAATCTNCGNACCAACAA |
| EV71-2800F+ | TTCACNTACATGCGCTTTGANGC |
| EV71-A2− | CCATCGATGGTTTTTTTTTTTTTTTTTTTTTTTTTTGCTATTCTGG |
| *Mlu*I-vec+ | TCAAACGCGTTTGAAGACGAAAGGGCCTCG |
| *Pvu*T7-45+ | AAATTCGATCGAAATTAATACGACTCACTATAGGTTAAAACAGCCTGTGGGTTGCA-CCCACTCACAGGGCCCACTGGGC |
| S472+ | GAATGCGGTTAATTCTAACTGCGGAGCAC |
| S472− | GTGCTCCGCAGTTAGAATTAACCGCATTC |
| S480+ | CCTAACTGCGGGGCACATACCCT |
| S480− | AGGGTATGTGCCCCGCAGTTAGG |
| S481+ | CCTAACTGCGGAACACATACCCTTAATC |
| S481− | GATTAAGGGTATGTGTTCCGCAGTTAGG |
| *Sna*BI-vec− | AAATTACGTAATTTCGATAAGCCAGTCGAG |
| *Sna*BI-T7-EV71+ | TTAATACGTATTAATACGACTCACTATAGGTTAAAACAGCCTGTGGGTTGCACC |
| TR2784+ | GACATAACCGGTTATGCGCAGATGCGC |
| TR2784− | GCGCATCTGCGCATAACCGGTTATGTC |
| TR5000F+ | ATAGCGTCGACACCGTGGTATCGG |
| tr-6300R− | AGGATGTGTCTTTTCTTGATGCCC |

RT-PCR with primers *Sna*BI-T7-EV71+ and 1595R− and then cloned into pEV71(BrCr-TR) after partial digestion with *Sna*BI and *Bam*HI. This cDNA clone was designated pts-TR. For the construction of a cDNA clone of EV71(ts-ts-TR), a DNA fragment was obtained from the EV71(BrCr-ts) viral genome by RT-PCR with primers EV71-1500F+ and 3564− and then cloned into pts-TR after partial digestion with *Xma*I and *Bam*HI. This cDNA clone of mutant ts-ts-TR was designated pts-ts-TR. For the construction of a cDNA clone of EV71(BrCr-ts), a DNA fragment was obtained from the EV71(BrCr-ts) viral genome by RT-PCR with primers EV71-1500F+ and A2*Bam*HI− and then cloned into pts-ts-TR after digestion with *Xma*I and *Spe*I. This cDNA clone of mutant EV71(BrCr-ts) was designated pEV71(BrCr-ts). cDNA clones of EV71(ts2784) and EV71(TR2784) were prepared by site-directed mutagenesis by PCR with primers 2784+ and 2784− or with primers TR2784+ and TR2784−, using pEV71(BrCr-TR) or pEV71(BrCr-ts) as the template.

Next, we constructed cDNA clones of other *ts* mutants by introducing the corresponding mutations of the attenuation and *ts* determinants of PV Sabin strains (Fig. 3). For the construction of a cDNA clone of EV71(3′), site-directed mutagenesis was performed by PCR with primers 6153C+ and 6153C−, using pEV71(BrCr-TR) as the template. The clone obtained was subjected to site-directed mutagenesis with primers 7023AT+ and 7023AT−. Next, a DNA fragment was obtained by PCR with primers TR5000F+ and 7409G−, using the obtained clone as the template, and then cloned into pEV71(BrCr-TR) following digestion with *Spe*I and *Mlu*I. This cDNA clone of EV71(3′) was designated pEV71(3′). A cDNA clone of EV71(S1-3′) was obtained by site-directed mutagenesis by PCR with primers S480+ and S480−, using pEV71(3′) as the template. cDNA clones of EV71(S1), EV71(S2) and EV71(S3) were obtained by site-directed mutagenesis with primer set S480+ and S480−, with S481+ and S481− or with S472+ and S472−, respectively, using pEV71(BrCr-TR) as the template.

**RNA transfection.** RNA transcripts were obtained by using a RiboMAX large-scale RNA production system–T7 kit (Promega) with *Mlu*I-linearized DNA as the template. The *in vitro*-synthesized RNA transcripts were transfected onto the monolayer of Vero cells in six-well plates (Falcon) by the DEAE–dextran method and incubated at 35 °C in 2 ml 5% FCS/DMEM per well (Lu *et al.*, 1995). Cytopathic effects (CPE) on Vero cells were observed at 24 h post-transfection (p.t.). The cells were harvested when all of the cells exhibited CPE (4–7 days p.t.) and stored at −70 °C. The titres of recovered EV71 mutants were $10^5$–$10^6$ 50% cell culture infectious dose ($CCID_{50}$) $ml^{-1}$.

**Virus titration.** Virus titre was determined by measuring $CCID_{50}$ by the microtitration assay in Vero cells, as described previously

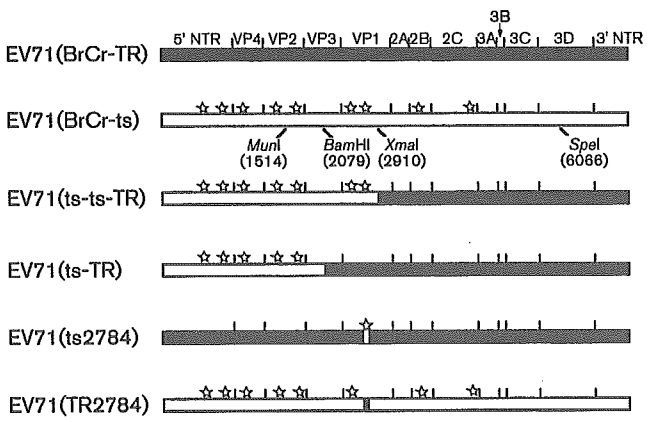


**Fig. 1.** Schematic diagram of the genomes of EV71 mutants. The sequences derived from the parental EV71(BrCr-TR) genome are represented as closed boxes and the sequences derived from the EV71(BrCr-ts) genome are represented as open boxes. The mutations observed in the EV71(BrCr-ts) genome are shown as open stars on each mutant genome. Restriction-enzyme sites are shown on the genome of EV71(BrCr-ts).

(Nagata *et al.*, 2002). Briefly, inoculated Vero cells were cultured at 36 °C for 10 days and observed for CPE. The value of $CCID_{50}$ was calculated according to the Behrens–Kärber method (Kärber, 1931).

**Growth kinetics of EV71 mutants.** Vero-cell monolayers were cultured in 96-well plates (Stripwell Plate; Corning) containing $2{\cdot}4 \times 10^4$ cells per well. EV71 mutants were inoculated into the cells at an m.o.i. of 1·0 ($2{\cdot}4 \times 10^4$ $CCID_{50}$ virus per well) and then incubated for 1 h at 36 °C. Inoculated cells were washed three times with 5 % FCS/DMEM and then 100 µl 5 % FCS/DMEM was added per well. The cells were incubated at 36 °C and harvested at the times indicated, from 2 to 12 h post-infection. The titre of virus was determined by $CCID_{50}$ measurement.

**Plaque assay.** The plaque assay was performed in 12-well plates (Falcon) containing a Vero-cell monolayer. Tenfold dilutions of virus solution were inoculated at 100 µl per well and incubated for 30 min at 36 °C. Then, 1 ml 2 % FCS/modified Eagle's medium (MEM) containing 0·5 % agarose ME (Iwai Kagaku) was added per well and incubated at 36 °C. After incubation for 4 days, 0·5 % agarose ME in 2 % FCS/MEM was overlaid on the first layer of agarose gel and further incubated for 3 days at 36 °C. The cells were fixed in formaldehyde and then stained with 0·5 % crystal violet.

**Temperature sensitivity.** The temperature sensitivity of viruses was evaluated by determining the virus titre in Vero cells at 36 °C, which we used for the isolation of EV71 from clinical samples, and at a supraoptimal temperature, 39 °C. Temperature sensitivity was expressed as logarithmic difference of the $CCID_{50}$ values at 36 and 39 °C ($\Delta CCID_{50}$). We defined temperature sensitivity from 2·0 to 2·75 logarithmic difference as a slight *ts* phenotype, and those with more than 2·75 logarithmic difference as a strong *ts* phenotype.

**Monkey neurovirulence test.** Eight 17–21-year-old female cynomolgus monkeys were used for the determination of neurovirulence of EV71 mutants. All animal procedures were approved by the Committee for Biosafety and Animal Handling and the Committee for Ethical Regulation of the National Institute of Infectious Diseases, Japan. Animal care, breeding, virus inoculation and observation were performed in accordance with the guidelines of the committees.

Under light anaesthesia with ketaral and xylazine, 1 ml of each virus solution (containing $10^7$ $CCID_{50}$ virus) was inoculated intravenously into the right tibial vein. Neurological manifestations of monkeys were checked daily for 10 days and autopsy was performed on day 10 post-inoculation (p.i.) after anaesthesia. Moribund monkeys before 10 days p.i. were sacrificed under deep anaesthesia. At autopsy, various parts of the central nervous system (CNS) were sampled for histopathological and virological analyses. The method of scoring the histological changes of the CNS (lesion score) was described previously (Nagata *et al.*, 2002). For virus isolation, a portion of excised tissues was stored at −80 °C. After freezing and thawing, 10 % (w/v) tissue homogenates in MEM containing 2 % FBS were centrifuged at 10 000 *g* for 10 min to remove cell debris. Supernatants were subjected to virus isolation in Vero cells. The cells were checked for CPE for 1 week and then blind passage was conducted for CPE-negative samples after freezing and thawing of the first-round passage. If CPE was not observed in the first- or second-round cultures, the result of virus isolation was recorded as negative.

## RESULTS

### Identification of the *ts* determinant of EV71(BrCr-ts)

To map the critical *ts* mutation of a *ts* variant of EV71 [EV71(BrCr-ts)], the entire genome sequence was determined and compared with that of a *tr* variant [EV71(BrCr-TR)]. The EV71(BrCr-ts) genome had nine nucleotide changes compared with that of EV71(BrCr-TR) and three of them were non-synonymous (Table 2). The three amino acid changes were located in capsid proteins VP2 and VP1 and in non-structural protein 2C (Table 2). We introduced these mutations into the infectious clone of EV71(BrCr-TR) to generate EV71 mutants, as described in Methods (Fig. 1). Viable viruses were recovered from all six clones, although their virus titres were different (Table 3).

To identify the *ts* determinant of EV71(BrCr-ts), temperature sensitivity was analysed for the parental and mutant

**Table 2.** Mutations of the EV71(BrCr-ts) genome

Mutations are from the BrCr-TR to the BrCr-ts genome.

| Nucleotide position | Site of mutation | Nucleotide change | Amino acid change |
|---|---|---|---|
| 491 | 5′ NTR | U to C | – |
| 681 | 5′ NTR | U to C | – |
| 848 | VP4 | C to U | – |
| 1154 | VP2 | U to C | – |
| 1707 | VP2 | G to A | Ala253 to Thr |
| 2693 | VP1 | U to C | – |
| 2784 | VP1 | U to C | Tyr116 to His |
| 4034 | 2B | A to G | – |
| 4990 | 2C | C to U | Thr305 to Ile |

**Table 3.** Temperature sensitivity of EV71 mutants

| EV71 mutant | Titre* at: | | Δ36/39 °C |
|---|---|---|---|
| | 36 °C | 39 °C | |
| BrCr-TR | 4·25 | 3·0 | 1·25 |
| ts-TR | 3·75 | 1·75 | 2·0 |
| ts-ts-TR | 2·5 | ND (<0·5) | >2·0 |
| BrCr-ts | 3·5 | ND (<0·5) | >3·0 |
| ts2784 | 3·25 | ND (<0·5) | >2·75 |
| TR2784 | 5·0 | 3·0 | 2·0 |
| S1 | 4·25 | 2·25 | 2·0 |
| S2 | 4·0 | 1·75 | 2·25 |
| S3 | 3·5 | 1·25 | 2·25 |
| 3′ | 4·0 | ND (<0·5) | >3·5 |
| S1-3′ | 4·0 | ND (<0·5) | >3·5 |
| 3′ (4511, spinal cord) | 4·0 | ND (<0·5) | >3·5 |
| 3′ (4511, brainstem) | 4·13 | ND (<0·5) | >3·6 |
| 3′ (4512, brainstem) | 4·0 | ND (<0·5) | >3·5 |
| S1-3′ (4514, spinal cord) | 4·13 | ND (<0·5) | >3·6 |

*Virus titre represents $\log_{10}(CCID_{50})$ in 10 μl virus sample.
ND, Not detected.

viruses by measuring the virus titre at 36 and 39 °C. Although the virus titres of EV71(ts2784) and EV71(ts-ts-TR) were much lower than that of the cDNA-derived EV71(BrCr-TR), even at 36 °C, the two mutants did not grow at 39 °C as well as EV71(BrCr-ts) (Table 3).

Introduction of a single nucleotide substitution at nt 2784 (U to C) into the EV71(BrCr-TR) genome resulted in impaired virus growth at 39 °C (Δ36/39 °C, >2·75 log) (Table 3). In contrast, a reciprocal substitution (C to U) at the same position of the EV71(BrCr-ts) genome resulted in only a slight *ts* phenotype [mutant EV71(TR2784); Δ36/39 °C, 2·0 log]. The plaque sizes of EV71(BrCr-TR) (cDNA-derived), EV71(ts-TR) and EV71(TR2784) were similar to that of the parental strain (Fig. 2a). On the other hand, EV71(ts-ts-TR) and EV71(ts2784) viruses showed smaller plaques, as well as EV71(BrCr-ts). These results indicate that a single nucleotide substitution at nt 2784 (VP1-Tyr116) is mainly responsible for both the *ts* and small-plaque phenotypes of EV71(BrCr-ts).

## Construction of EV71 mutants carrying the *ts* determinants of PV Sabin strains

To generate *ts* mutants that could show growth comparable with that of the parental strain *in vitro*, we examined the effect of the *ts* determinants of PV Sabin strains. As illustrated in Fig. 3, we constructed a series of EV71(BrCr) mutants carrying corresponding nucleotide substitutions.

Firstly, we focused on the mutations in the 5′ non-translated region (NTR) within domain V of the genomes of Sabin strains (at nt 480, 481 and 472 for Sabin 1, 2 and 3, respectively; Fig. 3c), which act as a *ts* determinant and also as the major determinant of attenuation. The 5′ NTR of the EV71(BrCr) genome had a type I internal ribosome entry

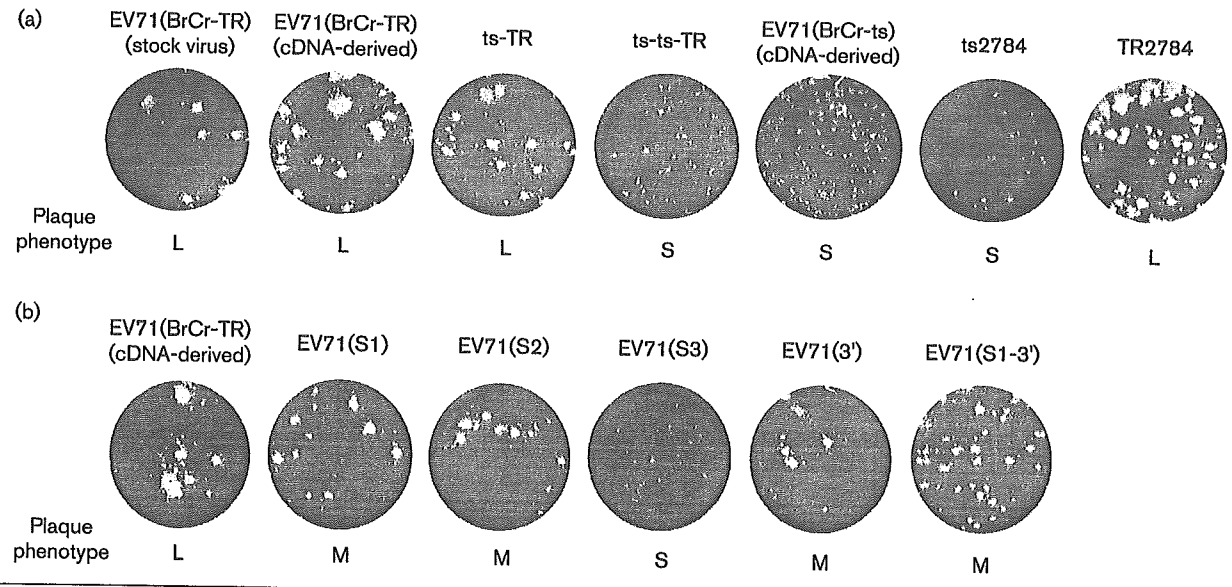


**Fig. 2.** Plaque phenotype of EV71 mutants. (a) Plaque phenotype of EV71 mutants derived from EV71(BrCr-ts). (b) Plaque phenotype of EV71 mutants carrying mutations of Sabin strains. Mutants EV71(S1), EV71(S2) and EV71(S3) have a mutation of the 5′ NTR of Sabin 1, 2 or 3, respectively. The EV71(3′) mutant has mutations in the $3D^{pol}$-coding region and 3′ NTR. The EV71(S1-3′) mutant contains all the mutations of the EV71(S1) and of EV71(3′) mutants. The assay was performed on Vero-cell monolayers incubated at 36 °C. L, Large-plaque phenotype; M, medium-plaque phenotype; S, small-plaque phenotype.

(a)

| | PV1 (Mahoney) | PV1 (Sabin) | EV71 (BrCr) |
|---|---|---|---|
| 5′ NTR | A(480) | G(480) | A(485) |
| $3D^{pol}$ | Tyr(73) | His(73) | Tyr(73) |
| $3D^{pol}$ | Thr(362) | Ile(362) | Cys(363) |
| 3′ NTR | A(7441) | G(7441) | A(7409) |

(b)

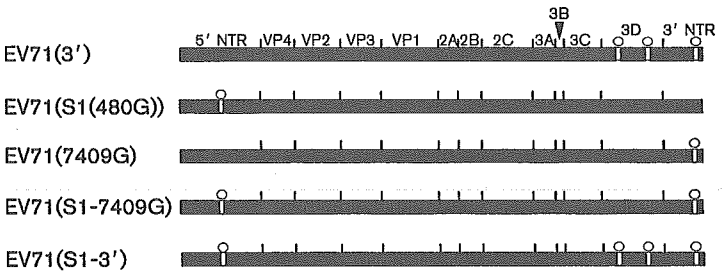


(c)

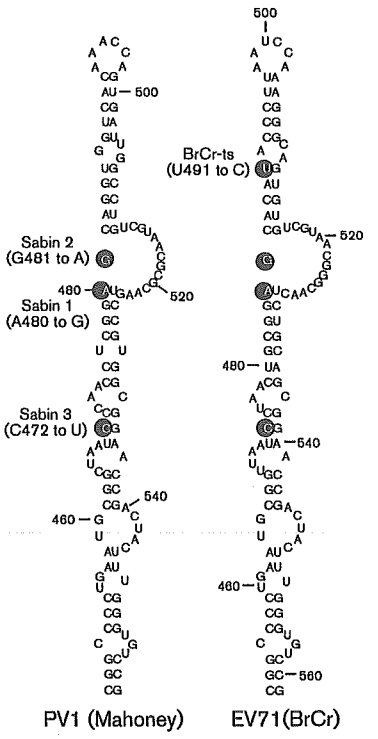


(d)

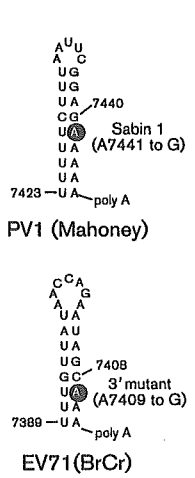


**Fig. 3.** EV71 mutants containing the corresponding mutations of the *ts* determinants of PV Sabin strains. (a) *ts* determinants of Sabin 1 introduced into the EV71(BrCr-TR) genome. The corresponding sites of the EV71(BrCr-TR) genome were substituted to those of Sabin 1. Numbers in parentheses represent the nucleotide position of the mutations on the genomes (5′ NTR and 3′ NTR) or the position of amino acids on the $3D^{pol}$ protein. (b) Schematic diagram of the genomes of EV71 mutants. Sequences derived from the parental EV71(BrCr-TR) genome are represented as closed boxes and mutations derived from the Sabin 1 genome are represented as open boxes with open circles. EV71 mutants carrying mutations of Sabin 2 or 3 in the 5′ NTR [mutants EV71(S2) and EV71(S3), respectively] are not shown. (c) RNA secondary-structure model of domain V in the IRES of PV1(Mahoney) and EV71(BrCr-TR), proposed by Pilipenko *et al.* (1989). (d) RNA structural models of the 3′ NTR of PV1(Mahoney) and that of EV71(BrCr-TR), obtained by the MFOLD 3.1 program (http://www.bioinfo.rpi.edu/applications/mfold/). The position of a *ts* determinant of Sabin 1 (G7441) and the corresponding site of the EV71(BrCr-TR) genome (A7409) are shown in closed circles.

site (IRES) activity, like that of the PV genome, and its structure model revealed an RNA secondary structure that was typical of the enterovirus IRES (Thompson & Sarnow, 2003). In a predicted secondary-structure model of domain V of the EV71(BrCr) genome, nt 485, 486 and 474 corresponded to the mutations of Sabin 1, 2 and 3, respectively (Fig. 3c).

Secondly, mutations corresponding to the major *ts* determinants of Sabin 1 in the 3D polymerase ($3D^{pol}$)-coding region and 3′ NTR were introduced into the infectious clone of EV71(BrCr-TR). The locations of the triple mutations in the EV71(BrCr-TR) genome (Tyr-73 and Cys-363 in $3D^{pol}$ and 7409A in the 3′ NTR) were predicted from the amino acid or nucleotide sequence alignment between EV71(BrCr-TR) and Sabin 1 (Fig. 3a).

As shown in Fig. 2(b), all mutants except the EV71(S3) mutant formed medium-sized plaques, which were smaller than those of the parental strain, but larger than those of the EV71(S3) mutant. The EV71(S3) mutant showed small-sized plaques, similar to those of the BrCr-ts variant. A PV1 mutant carrying a mutation of the 5′ NTR of the Sabin 3 genome showed a significant reduction in virus growth (Malnou *et al.*, 2003).

Next, we examined the temperature sensitivity of EV71 mutants by measuring the virus titre in Vero cells at 36 or 39 °C (Table 3). The results indicated that mutations in the 5′ NTR [EV71(S1) mutant] were involved in a slight *ts* phenotype (Δ36/39 °C, 2·0 log) and that triple mutations in the $3D^{pol}$-coding region and the 3′ NTR [EV71(3′) mutant] conferred a strong *ts* phenotype to EV71(BrCr-TR) (Δ36/39 °C, >3·5 log) (Table 3). Therefore, the triple mutations in the $3D^{pol}$-coding region and 3′ NTR could serve as the strong *ts* determinants in the genetic context of EV71(BrCr-TR), as well as in the Sabin 1 genome.

*In vitro* growth kinetics of three EV71 mutants that were

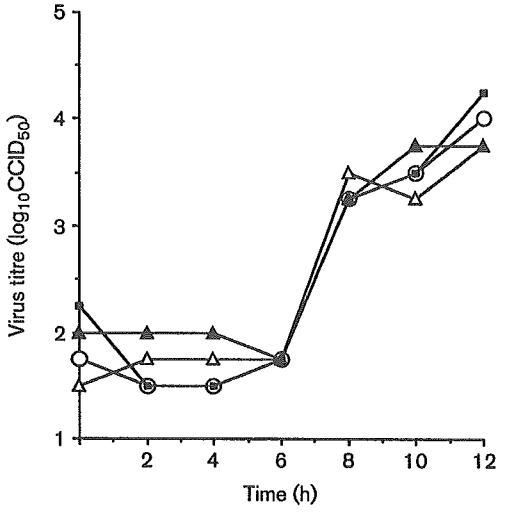


**Fig. 4.** Growth kinetics of EV71 mutants (BrCr-TR, ○; TR2784, ■; 3′, △; S1-3′, ▲).

used for the neurovirulence test in monkeys (see below) were measured in Vero cells at 36 °C (Fig. 4). All of the mutants showed growth kinetics similar to those of the parental EV71(BrCr-TR) strain.

The above results indicated that the introduction of *ts* mutations of the Sabin 1 genome into the 5′ NTR, 3D$^{Pol}$ coding region and 3′ NTR of the EV71(BrCr-TR) genome effectively generated *ts* mutants that retained *in vitro* growth kinetics comparable with those of the parental strain.

### Neurovirulence of EV71 mutants in cynomolgus monkeys

We determined the neurovirulence of cDNA-derived EV71 mutants in cynomolgus monkeys by intravenous inoculation. Two monkeys inoculated with $10^7$ $CCID_{50}$ of the cDNA-derived EV71(BrCr-TR) clone became moribund within 6 days p.i., similar to those inoculated with the parental EV71(BrCr-TR) strain (Nagata *et al.*, 2004). The cDNA-derived EV71(BrCr-TR) induced characteristic neurological manifestations, such as tremor and ataxia, from days 4 and 5 p.i., respectively (Table 4). In contrast, monkeys inoculated with the same dose of cDNA-derived mutants [EV71(TR2784), EV71(3′) and EV71(S1-3′)] showed mild neurological manifestations and histological changes. None of the six monkeys that were inoculated with EV71 mutants became moribund or showed ataxia within 10 days p.i. Moreover, mutant viruses in the CNS were detected in the spinal cord and in the brainstem, whilst the parental strain showed disseminated distribution (Nagata *et al.*, 2002). The total lesion scores of mutants were decreased (Table 4). For the infection of EV71(S1-3′), no viable virus was recovered from the CNS of an inoculated monkey on day 10 p.i. (monkey 4513) and the virus was only isolated from the spinal cord in another inoculated monkey (4514). Thus, the infection of EV71(S1-3′) resulted in the most limited clinical manifestations and in restricted distribution of the virus in the CNS.

To examine the selection pressure in the CNS of monkeys against the temperature sensitivity of EV71, we examined the *ts* phenotype of EV71(3′) and EV71(S1-3′) viruses recovered from the CNS of inoculated monkeys. All of the recovered viruses retained a strong *ts* phenotype, similar to that of the original EV71(3′) and EV71(S1-3′) viruses (Table 3). This suggests that the temperature sensitivity of EV71 is not the critical factor to achieve infection in the CNS of monkeys.

## DISCUSSION

The BrCr strain was isolated from an aseptic meningitis patient as the prototype strain of EV71 (Schmidt *et al.*, 1974). Its entire genome sequence is far from that of PV (Brown & Pallansch, 1995). Epidemiological analyses of

**Table 4.** Summary of the clinical manifestations of monkeys and virus isolation

| Virus | Monkey no. | Clinical manifestation* | | | Virus isolation | | | | Lesion score |
|---|---|---|---|---|---|---|---|---|---|
| | | Tremor | Ataxia | Moribund | Spinal cord | Brainstem | Cerebellum | Cerebrum | |
| EV71(BrCr-TR) | 4507 | Day 4 | Day 5 | Day 6 | + | + | + | + | 2·29 |
| | 4508 | Day 4 | Day 5 | Day 6 | + | + | + | + | 2·51 |
| EV71(TR2784) | 4509 | Day 7 | – | – | + | + | – | – | 0·78 |
| | 4510 | Day 6 | – | – | + | – | – | + | 0·72 |
| EV71(3′) | 4511 | Day 9 | – | – | + | + | – | – | 1·07 |
| | 4512 | Day 8 | – | – | – | + | – | – | 0·59 |
| EV71(S1-3′) | 4513 | Day 9 | – | – | – | – | – | – | 0·0 |
| | 4514 | Day 9 | – | – | + | – | – | – | 1·09 |

*Time post-inoculation when the monkey started to show the clinical manifestation is indicated. Monkeys were sacrificed at day 6 (for 4507 and 4508) or day 10 (for 4509, 4510, 4511, 4512, 4513 and 4514) post-inoculation.

EV71 revealed that the BrCr strain is not related closely to two major genogroups of EV71 (B and C); thus, it is the sole member of genogroup A (Brown *et al.*, 1999). Previous studies showed that cynomolgus monkeys inoculated with the BrCr strain exhibited typical neurological manifestations and histopathological legions after intraspinal or subcutaneous inoculation (Hashimoto & Hagiwara, 1983; Hashimoto *et al.*, 1978). Furthermore, a cell culture-selected *ts* variant of the BrCr strain [EV71(BrCr-ts)] had been generated (Hagiwara *et al.*, 1983; Hashimoto & Hagiwara, 1983) and was one of the initial candidates of attenuated EV71 strains. Therefore, we first examined this laboratory variant of the BrCr strain to generate attenuated EV71 strains.

To generate attenuated strains of EV71, we focused on temperature sensitivity as an *in vitro* marker. In general, temperature sensitivity of PV vaccine strains serves as an *in vitro* phenotypic marker of attenuation. However, the extent of temperature sensitivity does not necessarily correlate with the extent of attenuation of PV (Bouchard *et al.*, 1995; Christodoulou *et al.*, 1990; Georgescu *et al.*, 1995; Macadam *et al.*, 1989, 1991; Minor, 1992; Omata *et al.*, 1986). Moreover, the *ts* revertant could retain its attenuated phenotype, suggesting that there is no direct link between the arbitrary *ts* phenotype and attenuation (Rowe *et al.*, 2000). Thus, among the *ts* determinants, only some could serve as the attenuation determinants. We examined the genome of EV71(BrCr-ts) to identify the *ts* determinant that could be an initial candidate of the attenuation mutation. We identified a mutation at nt 2784 (VP1-Tyr116 to His) as the *ts* determinant of EV71(BrCr-ts). However, this mutation also conferred a small-plaque phenotype (Fig. 2a). Alignment of the amino acid sequences of EV71(BrCr-TR) and PV1(Mahoney) in the VP1 region suggests that the corresponding amino acids of PV1(Mahoney) would be Thr115, which is located near an interface of protomers between the adjoining VP1, via Gln233 of VP3 (Hogle *et al.*, 1985). Tyr116 of the BrCr-ts strain is located in a region of VP1 that is highly conserved among different EV71 strains (data not shown). One of the attenuation determinants of Sabin 3 is located in the capsid protein (Phe91 of VP3) near an interface between protomers (Minor *et al.*, 1989; Westrop *et al.*, 1989) and affects the virus-assembly process in a temperature-dependent manner (Minor *et al.*, 1989). Therefore, we could not obtain *ts* mutants with a growth activity comparable with that of the parental strain by utilizing the *ts* determinant of EV71(BrCr-ts).

We examined the effect of the *ts* determinants of Sabin strains on the temperature sensitivity of EV71. We focused on *ts* determinants of Sabin 1 that are located in structurally and functionally conserved regions among enteroviruses, i.e. the 5′ NTR, $3D^{Pol}$ and 3′ NTR (Kawamura *et al.*, 1989; Omata *et al.*, 1986). Between PV and EV71, the predicted secondary structures of 5′ NTR and 3′ NTR are highly conserved (Fig. 3). Mutations in the 5′ NTR of Sabin strains cause a reduction in the IRES activity (Muzychenko *et al.*, 1991; Svitkin *et al.*, 1985, 1988, 1990) and act as a *ts* determinant, as well as the major attenuation determinant (Bouchard *et al.*, 1995; Christodoulou *et al.*, 1990; Evans *et al.*, 1985; Georgescu *et al.*, 1995; Macadam *et al.*, 1989, 1991; Minor, 1992; Omata *et al.*, 1986). The attenuation determinant in the 5′ NTR of Sabin 3 leads to translation defects in neuronal and non-neuronal organs *in vivo* (Kauder & Racaniello, 2004). However, in PV1 infection, the reduced level of translation was not the main determinant of attenuation (Arita *et al.*, 2004). Therefore, the mechanism of the attenuation effect of the mutations in the 5′ NTR of Sabin strains remained to be further elucidated.

The mutation of nt 6203 (His73 of the $3D^{Pol}$ protein) affects the oligomerization and uridylylation of viral protein $3B^{VPg}$ in a temperature-sensitive manner (Paul *et al.*, 2000). Another mutation of nt 7071(Ile362 of the $3D^{Pol}$ protein) is required for the *ts* phenotype of Sabin 1 (Georgescu *et al.*, 1995). The amino acid residue at 362 of the $3D^{Pol}$ protein is located at interface I of $3D^{Pol}$ (Hansen *et al.*, 1997); together with the mutation of nt 6203, this amino acid residue may also affect the oligomerization of the $3D^{Pol}$ protein. The mutation in the 3′ NTR, which is located in a stem–loop structure (Fig. 3d), has been suggested to have an effect on the *ts* phenotype, along with other mutations of $3D^{Pol}$ (Georgescu *et al.*, 1995) or the mutation in the 5′ NTR (Christodoulou *et al.*, 1990), by an unknown mechanism. EV71 mutants with mutations in the $3D^{Pol}$-coding region and 3′ NTR showed a strong *ts* phenotype, in contrast to a slight *ts* phenotype that was caused by mutations in the 5′ NTR (Table 3). These results indicate that EV71 and PV1 share common genetic determinants of temperature sensitivity, based at least in part on the conserved replication machinery.

We examined the neurovirulence of EV71 mutants by intravenous inoculation into cynomolgus monkeys. The inoculation route is a critical factor for neurological disorders of EV71 infection in the monkey model. After intraspinal inoculation of the BrCr strain, monkeys showed flaccid paralysis, but not tremor or ataxia, due to intraspinal spread of the virus (Nagata *et al.*, 2004). Therefore, we applied an intravenous inoculation model to avoid direct involvement of the inoculated virus in the CNS, which would not occur in the natural course of EV71 infection.

All three EV71 mutants caused mild neurological symptoms in monkeys after intravenous inoculation, but did not cause lethal neurological disorders that were observed in infection with EV71(BrCr-TR) (Table 4). Interestingly, mutant EV71(TR2784) had only a minor *ts* phenotype, but showed a slightly attenuated phenotype. Infections caused by EV71(TR2784) or EV71(3′), which showed a strong *ts* phenotype, resulted in a similar lesion score, despite their different temperature sensitivity. Therefore, temperature sensitivity could not serve as an absolute indicator of the attenuated neurovirulence of EV71. The distribution of EV71 mutants in the CNS was also restricted, compared

with that of the parental strain. Among the mutants examined, EV71(S1-3′) resulted in the most limited clinical manifestations and in a restricted distribution of the virus in the CNS. A cumulative effect of the mutations in the 5′ NTR and $3D^{pol}$-coding region on the attenuation of PV has been reported (Tardy-Panit *et al.*, 1993). However, infection by EV71(S1-3′) was still associated with minor neurological symptoms in inoculated monkeys and virus was isolated from the spinal cord. Thus, mutation of Sabin 1 in the 5′ NTR could not completely suppress infection by EV71 in the spinal cord of monkeys inoculated by the intravenous route. This observation might suggest that the spinal cord serves as a preferred site of infection for both PV and EV71 (Arita *et al.*, 2004). However, because of the different mechanisms of pathogenesis, the effect of mutations of Sabin 1 on the infection of EV71 remain to be further elucidated.

EV71 antigen was detected in the early phase of infection, followed by clinical manifestations, in monkeys (Nagata *et al.*, 2002). It was possible that EV71 mutants replicated in the CNS in a disseminated manner, as well as the parental virulent strain, in the early phase of infection. Therefore, the tissue specificity of EV71 mutants in the CNS remains to be further studied.

In conclusion, we have generated a cDNA-derived virulent strain of EV71 that maintained the *in vitro* and *in vivo* phenotypes of a neurovirulent strain, EV71(BrCr-TR). Based on this infectious cDNA clone of EV71, we identified several molecular determinants conferring *ts* and attenuated phenotypes to EV71. The cDNA-derived virulent and attenuated strains of EV71 should serve as a valuable tool for the elucidation of EV71-induced severe neurological disorders and development of a vaccine strain.

## ACKNOWLEDGEMENTS

We are grateful to Ms A. Harashima, Ms Y. Sato and Ms J. Wada for their excellent assistance. This work was supported by grants-in-aid from the Japan Society for Promotion of Science and from the Ministry of Health, Labour and Welfare, and by a grant for health research from the Regional Office for the Western Pacific, World Health Organization.

## REFERENCES

**Abubakar, S., Chee, H. Y., Shafee, N., Chua, K. B. & Lam, S. K. (1999).** Molecular detection of enteroviruses from an outbreak of hand, foot and mouth disease in Malaysia in 1997. *Scand J Infect Dis* **31**, 331–335.

**Ahmad, K. (2000).** Hand, foot, and mouth disease outbreak reported in Singapore. *Lancet* **356**, 1338.

**Arita, M., Shimizu, H. & Miyamura, T. (2004).** Characterization of *in vitro* and *in vivo* phenotypes of poliovirus type 1 mutants with reduced viral protein synthesis activity. *J Gen Virol* **85**, 1933–1944.

**Bouchard, M. J., Lam, D.-H. & Racaniello, V. R. (1995).** Determinants of attenuation and temperature sensitivity in the type 1 poliovirus Sabin vaccine. *J Virol* **69**, 4972–4978.

**Brown, B. A. & Pallansch, M. A. (1995).** Complete nucleotide sequence of enterovirus 71 is distinct from poliovirus. *Virus Res* **39**, 195–205.

**Brown, B. A., Oberste, M. S., Alexander, J. P., Jr, Kennett, M. L. & Pallansch, M. A. (1999).** Molecular epidemiology and evolution of enterovirus 71 strains isolated from 1970 to 1998. *J Virol* **73**, 9969–9975.

**Chan, L. G., Parashar, U. D., Lye, M. S. & 9 other authors (2000).** Deaths of children during an outbreak of hand, foot, and mouth disease in Sarawak, Malaysia: clinical and pathological characteristics of the disease. *Clin Infect Dis* **31**, 678–683.

**Chen, Y.-C., Yu, C.-K., Wang, Y.-F., Liu, C.-C., Su, I.-J. & Lei, H.-Y. (2004).** A murine oral enterovirus 71 infection model with central nervous system involvement. *J Gen Virol* **85**, 69–77.

**Christodoulou, C., Colbere-Garapin, F., Macadam, A., Taffs, L. F., Marsden, S., Minor, P. & Horaud, F. (1990).** Mapping of mutations associated with neurovirulence in monkeys infected with Sabin 1 poliovirus revertants selected at high temperature. *J Virol* **64**, 4922–4929.

**Chumakov, M., Voroshilova, M., Shindarov, L. & 16 other authors (1979).** Enterovirus 71 isolated from cases of epidemic poliomyelitis-like disease in Bulgaria. *Arch Virol* **60**, 329–340.

**Evans, D. M., Dunn, G., Minor, P. D., Schild, G. C., Cann, A. J., Stanway, G., Almond, J. W., Currey, K. & Maizel, J. V., Jr (1985).** Increased neurovirulence associated with a single nucleotide change in a noncoding region of the Sabin type 3 poliovaccine genome. *Nature* **314**, 548–550.

**Fujimoto, T., Chikahira, M., Yoshida, S., Ebira, H., Hasegawa, A., Totsuka, A. & Nishio, O. (2002).** Outbreak of central nervous system disease associated with hand, foot, and mouth disease in Japan during the summer of 2000: detection and molecular epidemiology of enterovirus 71. *Microbiol Immunol* **46**, 621–627.

**Georgescu, M. M., Tardy-Panit, M., Guillot, S., Crainic, R. & Delpeyroux, F. (1995).** Mapping of mutations contributing to the temperature sensitivity of the Sabin 1 vaccine strain of poliovirus. *J Virol* **69**, 5278–5286.

**Hagiwara, A., Yoneyama, T. & Hashimoto, I. (1983).** Isolation of a temperature-sensitive strain of enterovirus 71 with reduced neurovirulence for monkeys. *J Gen Virol* **64**, 499–502.

**Hansen, J. L., Long, A. M. & Schultz, S. C. (1997).** Structure of the RNA-dependent RNA polymerase of poliovirus. *Structure* **5**, 1109–1122.

**Hashimoto, I. & Hagiwara, A. (1983).** Comparative studies on the neurovirulence of temperature-sensitive and temperature-resistant viruses of enterovirus 71 in monkeys. *Acta Neuropathol* **60**, 266–270.

**Hashimoto, I., Hagiwara, A. & Kodama, H. (1978).** Neurovirulence in cynomolgus monkeys of enterovirus 71 isolated from a patient with hand, foot and mouth disease. *Arch Virol* **56**, 257–261.

**Herrero, L. J., Lee, C. S. M., Hurrelbrink, R. J., Chua, B. H., Chua, K. B. & McMinn, P. C. (2003).** Molecular epidemiology of enterovirus 71 in peninsular Malaysia, 1997–2000. *Arch Virol* **148**, 1369–1385.

**Ho, M., Chen, E.-R., Hsu, K.-H., Twu, S.-J., Chen, K.-T., Tsai, S.-F., Wang, J.-R. & Shih, S.-R. (1999).** An epidemic of enterovirus 71 infection in Taiwan. *N Engl J Med* **341**, 929–935.

**Hogle, J. M., Chow, M. & Filman, D. J. (1985).** Three-dimensional structure of poliovirus at 2·9 Å resolution. *Science* **229**, 1358–1365.

**Horie, H., Koike, S., Kurata, T. & 11 other authors (1994).** Transgenic mice carrying the human poliovirus receptor: new animal model for study of poliovirus neurovirulence. *J Virol* **68**, 681–688.

**Kärber, G. (1931).** Beitrag zur kollektiven Behandlung pharmakologischer Reihenversuche. *Arch Exp Pathol Pharmakol* **162**, 480–483 (in German).

**Kauder, S. E. & Racaniello, V. R. (2004).** Poliovirus tropism and attenuation are determined after internal ribosome entry. *J Clin Invest* **113**, 1743–1753.

**Kawamura, N., Kohara, M., Abe, S., Komatsu, T., Tago, K., Arita, M. & Nomoto, A. (1989).** Determinants in the 5′ noncoding region of poliovirus Sabin 1 RNA that influence the attenuation phenotype. *J Virol* **63**, 1302–1309.

**Koike, S., Horie, H., Sato, Y., Ise, I., Taya, C., Nomura, T., Yoshioka, I., Yonekawa, H. & Nomoto, A. (1993).** Poliovirus-sensitive transgenic mice as a new animal model. *Dev Biol Stand* **78**, 101–107.

**Komatsu, H., Shimizu, Y., Takeuchi, Y., Ishiko, H. & Takada, H. (1999).** Outbreak of severe neurologic involvement associated with enterovirus 71 infection. *Pediatr Neurol* **20**, 17–23.

**Kuo, R.-L., Kung, S.-H., Hsu, Y.-Y. & Liu, W.-T. (2002).** Infection with enterovirus 71 or expression of its 2A protease induces apoptotic cell death. *J Gen Virol* **83**, 1367–1376.

**Li, M.-L., Hsu, T.-A., Chen, T.-C., Chang, S.-C., Lee, J.-C., Chen, C.-C., Stollar, V. & Shih, S.-R. (2002).** The 3C protease activity of enterovirus 71 induces human neural cell apoptosis. *Virology* **293**, 386–395.

**Lin, T.-Y., Twu, S.-J., Ho, M.-S., Chang, L.-Y. & Lee, C.-Y. (2003).** Enterovirus 71 outbreaks, Taiwan: occurrence and recognition. *Emerg Infect Dis* **9**, 291–293.

**Lu, H.-H., Alexander, L. & Wimmer, E. (1995).** Construction and genetic analysis of dicistronic polioviruses containing open reading frames for epitopes of human immunodeficiency virus type 1 gp120. *J Virol* **69**, 4797–4806.

**Lu, C.-Y., Lee, C.-Y., Kao, C.-L. & 8 other authors (2002).** Incidence and case-fatality rates resulting from the 1998 enterovirus 71 outbreak in Taiwan. *J Med Virol* **67**, 217–223.

**Lum, L. C. S., Wong, K. T., Lam, S. K. & 7 other authors (1998).** Fatal enterovirus 71 encephalomyelitis. *J Pediatr* **133**, 795–798.

**Macadam, A. J., Arnold, C., Howlett, J. & 9 other authors (1989).** Reversion of the attenuated and temperature-sensitive phenotypes of the Sabin type 3 strain of poliovirus in vaccinees. *Virology* **172**, 408–414.

**Macadam, A. J., Pollard, S. R., Ferguson, G., Dunn, G., Skuce, R., Almond, J. W. & Minor, P. D. (1991).** The 5′ noncoding region of the type 2 poliovirus vaccine strain contains determinants of attenuation and temperature sensitivity. *Virology* **181**, 451–458.

**Mainou, C. E., Werner, A., Borman, A. M., Westhof, E. & Kean, K. M. (2003).** Effects of vaccine strain mutations in domain V of the internal ribosome entry segment compared in the wild type poliovirus type 1 context. *J Biol Chem* **279**, 10261–10269.

**McMinn, P. C. (2002).** An overview of the evolution of enterovirus 71 and its clinical and public health significance. *FEMS Microbiol Rev* **26**, 91–107.

**McMinn, P., Stratov, I. & Dowse, G. (1999).** Enterovirus 71 outbreak in Western Australia associated with acute flaccid paralysis. Preliminary report. *Commun Dis Intell* **23**, 199.

**McMinn, P., Lindsay, K., Perera, D., Chan, H. M., Chan, K. P. & Cardosa, M. J. (2001a).** Phylogenetic analysis of enterovirus 71 strains isolated during linked epidemics in Malaysia, Singapore, and Western Australia. *J Virol* **75**, 7732–7738.

**McMinn, P., Stratov, I., Nagarajan, L. & Davis, S. (2001b).** Neurological manifestations of enterovirus 71 infection in children during an outbreak of hand, foot, and mouth disease in Western Australia. *Clin Infect Dis* **32**, 236–242.

**Minor, P. D. (1992).** The molecular biology of poliovaccines. *J Gen Virol* **73**, 3065–3077.

**Minor, P. D., Dunn, G., Evans, D. M. A. & 8 other authors (1989).** The temperature sensitivity of the Sabin type 3 vaccine strain of poliovirus: molecular and structural effects of a mutation in the capsid protein VP3. *J Gen Virol* **70**, 1117–1123.

**Muzychenko, A. R., Lipskaya, G. Yu., Maslova, S. V., Svitkin, Y. V., Pilipenko, E. V., Nottay, B. K., Kew, O. M. & Agol, V. I. (1991).** Coupled mutations in the 5′-untranslated region of the Sabin poliovirus strains during in vivo passages: structural and functional implications. *Virus Res* **21**, 111–122.

**Nagata, N., Shimizu, H., Ami, Y. & 7 other authors (2002).** Pyramidal and extrapyramidal involvement in experimental infection of cynomolgus monkeys with enterovirus 71. *J Med Virol* **67**, 207–216.

**Nagata, N., Iwasaki, T., Ami, Y. & 8 other authors (2004).** Differential localization of neurons susceptible to enterovirus 71 and poliovirus type 1 in the central nervous system of cynomolgus monkeys after intravenous inoculation. *J Gen Virol* **85**, 2981–2989.

**Omata, T., Kohara, M., Kuge, S. & 8 other authors (1986).** Genetic analysis of the attenuation phenotype of poliovirus type 1. *J Virol* **58**, 348–358.

**Paul, A. V., Mugavero, J., Yin, J., Hobson, S., Schultz, S., van Boom, J. H. & Wimmer, E. (2000).** Studies on the attenuation phenotype of polio vaccines: poliovirus RNA polymerase derived from Sabin type 1 sequence is temperature sensitive in the uridylylation of VPg. *Virology* **272**, 72–84.

**Pilipenko, E. V., Blinov, V. M., Romanova, L. I., Sinyakov, A. N., Maslova, S. V. & Agol, V. I. (1989).** Conserved structural domains in the 5′-untranslated region of picornaviral genomes: an analysis of the segment controlling translation and neurovirulence. *Virology* **168**, 201–209.

**Pulli, T., Koskimies, P. & Hyypiä, T. (1995).** Molecular comparison of coxsackie A virus serotypes. *Virology* **212**, 30–38.

**Ren, R., Costantini, F., Gorgacz, E. J., Lee, J. J. & Racaniello, V. R. (1990).** Transgenic mice expressing a human poliovirus receptor: a new model for poliomyelitis. *Cell* **63**, 353–362.

**Rowe, A., Ferguson, G. L., Minor, P. D. & Macadam, A. J. (2000).** Coding changes in the poliovirus protease 2A compensate for 5′NCR domain V disruptions in a cell-specific manner. *Virology* **269**, 284–293.

**Sambrook, J. & Russell, D. (2001).** *Molecular Cloning: a Laboratory Manual*, 3rd edn, pp. 13.19–13.25. Cold Spring Harbor, NY: Cold Spring Harbor Laboratory.

**Schmidt, N. J., Lennette, E. H. & Ho, H. H. (1974).** An apparently new enterovirus isolated from patients with disease of the central nervous system. *J Infect Dis* **129**, 304–309.

**Shimizu, H., Utama, A., Yoshii, K. & 13 other authors (1999).** Enterovirus 71 from fatal and nonfatal cases of hand, foot and mouth disease epidemics in Malaysia, Japan and Taiwan in 1997-1998. *Jpn J Infect Dis* **52**, 12–15.

**Svitkin, Y. V., Maslova, S. V. & Agol, V. I. (1985).** The genomes of attenuated and virulent poliovirus strains differ in their *in vitro* translation efficiencies. *Virology* **147**, 243–252.

**Svitkin, Y. V., Pestova, T. V., Maslova, S. V. & Agol, V. I. (1988).** Point mutations modify the response of poliovirus RNA to a translation initiation factor: a comparison of neurovirulent and attenuated strains. *Virology* **166**, 394–404.

**Svitkin, Y. V., Cammack, N., Minor, P. D. & Almond, J. W. (1990).** Translation deficiency of the Sabin type 3 poliovirus genome: association with an attenuating mutation C472→U. *Virology* **175**, 103–109.

**Tardy-Panit, M., Blondel, B., Martin, A., Tekaia, F., Horaud, F. & Delpeyroux, F. (1993).** A mutation in the RNA polymerase of poliovirus type 1 contributes to attenuation in mice. *J Virol* **67**, 4630–4638.

**Thompson, S. R. & Sarnow, P. (2003).** Enterovirus 71 contains a type I IRES element that functions when eukaryotic initiation factor eIF4G is cleaved. *Virology* **315**, 259–266.

**Wang, J.-R., Tuan, Y.-C., Tsai, H.-P., Yan, J.-J., Liu, C.-C. & Su, I. J. (2002).** Change of major genotype of enterovirus 71 in outbreaks of hand-foot-and-mouth disease in Taiwan between 1998 and 2000. *J Clin Microbiol* **40**, 10–15.

**Wang, S.-M., Lei, H.-Y., Huang, K.-J., Wu, J.-M., Wang, J.-R., Yu, C.-K., Su, I.-J. & Liu, C.-C. (2003).** Pathogenesis of enterovirus 71 brainstem encephalitis in pediatric patients: roles of cytokines and cellular immune activation in patients with pulmonary edema. *J Infect Dis* **188**, 564–570.

**Wang, Y.-F., Chou, C.-T., Lei, H.-Y. & 8 other authors (2004).** A mouse-adapted enterovirus 71 strain causes neurological disease in mice after oral infection. *J Virol* **78**, 7916–7924.

**Westrop, G. D., Wareham, K. A., Evans, D. M. A. & 8 other authors (1989).** Genetic basis of attenuation of the Sabin type 3 oral poliovirus vaccine. *J Virol* **63**, 1338–1344.

**Zhao, W. D., Lahser, F. C. & Wimmer, E. (2000).** Genetic analysis of a poliovirus/hepatitis C virus (HCV) chimera: interaction between the poliovirus cloverleaf and a sequence in the HCV 5′ nontranslated region results in a replication phenotype. *J Virol* **74**, 6223–6226.

JOURNAL OF VIROLOGY, Apr. 2005, p. 4460–4469 Vol. 79, No. 7
0022-538X/05/$08.00+0 doi:10.1128/JVI.79.7.4460–4469.2005


# The Alpha/Beta Interferon Response Controls Tissue Tropism and Pathogenicity of Poliovirus

Miki Ida-Hosonuma,[1] Takuya Iwasaki,[2] Tomoki Yoshikawa,[1,3] Noriyo Nagata,[3] Yuko Sato,[3] Tetsutaro Sata,[3] Mitsutoshi Yoneyama,[4] Takashi Fujita,[4] Choji Taya,[5] Hiromichi Yonekawa,[5] and Satoshi Koike[1]*

*Department of Microbiology & Immunology,[1] Tokyo Metropolitan Institute for Neuroscience, Department of Tumor Cell Research,[4] and Department of Laboratory Animal Sciences,[5] Tokyo Metropolitan Institute of Medical Sciences, Tokyo Metropolitan Organization for Medical Research, and Department of Pathology, National Institute of Infectious Diseases,[3] Tokyo, and Department of Pathology, Institute of Tropical Medicine, Nagasaki University, Nagasaki,[2] Japan*

Received 29 August 2004/Accepted 12 November 2004

**Poliovirus selectively replicates in neurons in the spinal cord and brainstem, although poliovirus receptor (PVR) expression is observed in both the target and nontarget tissues in humans and transgenic mice expressing human PVR (PVR-transgenic mice). We assessed the role of alpha/beta interferon (IFN) in determining tissue tropism by comparing the pathogenesis of the virulent Mahoney strain in PVR-transgenic mice and PVR-transgenic mice deficient in the alpha/beta IFN receptor gene (PVR-transgenic/*Ifnar* knockout mice). PVR-transgenic/*Ifnar* knockout mice showed increased susceptibility to poliovirus. After intravenous inoculation, severe lesions positive for the poliovirus antigen were detected in the liver, spleen, and pancreas in addition to the central nervous system. These results suggest that the alpha/beta IFN system plays an important role in determining tissue tropism by protecting nontarget tissues that are potentially susceptible to infection. We subsequently examined the expression of IFN and IFN-stimulated genes (ISGs) in the PVR-transgenic mice. In the nontarget tissues, ISGs were expressed even in the noninfected state, and the expression level increased soon after poliovirus infection. On the contrary, in the target tissues, ISG expression was low in the noninfected state and sufficient response after poliovirus infection was not observed. The results suggest that the unequal IFN response is one of the important determinants for the differential susceptibility of tissues to poliovirus. We consider that poliovirus replication was observed in the nontarget tissues of PVR-transgenic/*Ifnar* knockout mice because the IFN response was null in all tissues.**

The replication of many viruses is restricted to certain cells and tissues in the host. This tissue tropism results in a distinct disease pattern unique for each virus. Since virus infection initiates after binding of the virion to a receptor on the cell surface, cellular receptors for viruses have been considered the primary determinants of tissue tropism. However, following the identification of receptors for a number of viruses, it became apparent that receptor distribution in the host is wider than the virus replication sites (38). This indicates that virus tropism may be determined by another factor(s) in addition to the virus receptor.

Poliovirus, belonging to the genus *Picornaviridae*, is the causative agent of an acute human central nervous system disease, poliomyelitis (33). After poliovirus infection, the virus first multiplies in the oropharyngeal and intestinal mucosa and then in the lymphatic tissues, such as the tonsils and Peyer's patches. The virus drains into the blood and circulates within the body. Because visceral tissues, except for adipose tissues, seem to be nonpermissive for poliovirus infection, apparent pathological lesions are not observed in the nonneural tissues. Therefore, the site of virus multiplication during the viremic phase has not been identified. Finally, poliovirus reaches the central nervous system, which leads to the development of a paralytic disease in less than 1% of persons naturally infected with wild-type poliovirus (4, 23, 35). Even in the central nervous system, the poliovirus antigen, nerve cell changes, and inflammatory reactions are localized mainly in motor neurons in the anterior horn of the spinal cord and neurons in the brainstem. The brainstem as far as the hypothalamus and thalamus bears most of the cerebral pathological changes in poliomyelitis. The cerebral cortex (except for the motor cortex), basal ganglia (except occasionally for the globus pallidus), and the cerebellar cortex (except for the vermis) are rarely affected (2, 6). In terms of modern molecular biology, tissue tropism may be determined by interactions between host and viral factors. It is therefore important to elucidate the molecular mechanism responsible for tropism.

The poliovirus receptor (PVR) has been considered a major determinant of poliovirus tissue tropism (13). The molecular cloning of the human *PVR* gene was reported more than a decade ago (18, 24). With cultured cells, susceptibility of poliovirus infection completely correlates with the presence of functional PVR. However, in vivo, this rule is not always true. Analyses of PVR expression in humans revealed that there are many tissues, such as the liver and kidneys, that express PVR but are not involved in the infection (18, 24). Transgenic mice expressing the human *PVR* gene with its natural promoter (PVR-transgenic mice) were produced as a new animal model

* Corresponding author. Mailing address: Department of Microbiology & Immunology, Tokyo Metropolitan Institute for Neuroscience, Tokyo Metropolitan Organization for Medical Research, Musashidai, Fuchu-shi, Tokyo 183-8526, Japan. Phone: 81-42-325-3881. Fax: 81-42-321-8678. E-mail: koike@tmin.ac.jp.

for the study of poliovirus pathogenicity (21, 32). PVR-transgenic mice exhibited a paralytic disease that resembled human poliomyelitis after poliovirus infection. PVR mRNA was detected in all tissues of PVR-transgenic mice by Northern blot hybridization, although expression was restricted to certain cells, such as neurons in the central nervous system (20, 32) and Bowman's capsule and tubules in the kidney (32). PVR was also detected in the glomerulus in the kidney by immunofluorescent staining (15). These data suggest that PVR is necessary for poliovirus infection but may not be the sole determinant of tissue tropism (reviewed in reference 29). The results also suggest the existence of other factors that determine tissue tropism concomitantly with PVR expression. It is possible that host factors required for poliovirus replication are abundant only in target tissues or that host factors inhibiting virus replication are present in nontarget tissues.

To identify possible host factors, we produced another transgenic mouse strain in which there is ubiquitous PVR expression under the control of the CAG promoter (14). If we hypothesize that host factors required for poliovirus replication are present only in susceptible tissues, the distribution of poliovirus replication sites in the new transgenic mice would be the same as or wider than that in the transgenic mice previously produced, since the distribution of the PVR has broadened. However, after intracerebral infection, poliovirus propagated to a slight degree in neurons and glial and ependymal cells near the inoculation sites on day 1 postinfection (p.i.) but the virus titer decreased from day 2 p.i. without development of fatal encephalitis and poliomyelitis. After intraperitoneal and intravenous infection, no apparent signs of illness or virus replication were observed. It seemed to us that an unknown factor(s) that prevented virus replication and spreading was induced. This led us to hypothesize that an innate immune response, such as the production of interferon (IFN), may influence the pathogenesis of poliovirus.

Picornaviruses are sensitive to IFNs (7, 8, 25, 27, 49). IFN plays a central role in the innate immune antiviral response. Infected cells produce alpha/beta IFNs, which induce a number of genes, called IFN-stimulated genes (ISGs), that confer an antiviral state (36, 39, 41). In some viruses, including coxsackievirus and Theiler's virus, alpha/beta IFN plays an important role in the pathogenicity and tissue tropism of the virus (9, 10, 28, 34, 44). However, little is known about the role of alpha/beta IFNs in poliovirus pathogenesis.

Here we report the results of experiments that we conducted to assess the contribution of alpha/beta IFN in the pathogenesis of poliovirus infection with a PVR-transgenic mouse model (20, 21). PVR-transgenic mice were crossed with IFN-α/β receptor (IFNAR) knockout mice in which alpha/beta IFN signaling is disrupted (26). Poliovirus infection of the resulting PVR-transgenic/*Ifnar* knockout mice revealed that the IFN system is an important determinant of poliovirus tissue tropism and poliovirus pathogenesis.

## MATERIALS AND METHODS

**Cells, viruses, and mice.** African green monkey kidney (AGMK) cell line JVK-03 (19) was maintained in Eagle's minimal essential medium supplemented with 5% fetal bovine serum. The poliovirus type 1 Mahoney strain was obtained by transfection of in vitro-synthesized RNA from infectious cDNA clone pOM (40) into JVK-03 cells. Virus titer was determined by a plaque assay on JVK-03 cells. A transgenic mouse strain, ICR-PVRtg21 (20, 21), was backcrossed for 10 generations with C57BL/6 mice, and then N10 mice were mated to obtain homozygotes (PVR-transgenic mice). The mouse strain deficient in the *Ifnar* gene, A129 (26), was purchased from B&K Universal Limited (United Kingdom) with the permission of M. Aguet. A129 was backcrossed for five generations with C57BL/6 mice and then with PVR-transgenic mice for two generations. $PVR^{+/+}$ $Ifnar^{-/-}$ mice were obtained by intercrossing these PVR-transgenic/*Ifnar* knockout mice.

Until the infection experiments, mice were maintained in an animal facility free of the following pathogens: *Citrobacter rodentium*, *Corynebacterium kutscheri*, *Mycoplasma pulmonis*, *Pasteurella pneumotropica*, *Salmonella* spp., cilia-associated respiratory bacillus, *Helicobacter hepaticus*, *Pseudomonas aeruginosa*, *Clostridium piliforme*, *Mycoplasma pulmonis*, ectromelia virus, lymphocytic choriomeningitis virus, mouse hepatitis virus, Sendai virus (HVJ), EDIM virus (rotavirus), minute virus of mice, mouse encephalomyelitis virus, pneumonia virus of mice, mouse adenovirus, reovirus type 3, ectoparasites, intestinal protozoa, and pinworm. Six-week-old mice were used for the experiments. All experiments with mice were performed in accordance with the Guidelines for the Care and Use of Laboratory Animals of the Tokyo Metropolitan Institute for Neuroscience.

**Poliovirus infection in mice.** Poliovirus at the indicated doses was inoculated intracerebrally, intravenously, or intraperitoneally as described previously (21). The mice were observed daily for 3 weeks or sacrificed at the indicated time p.i. The 50% lethal dose ($LD_{50}$) was calculated by the method of Kärber (45). In poly(I):poly(C) [poly(I:C)] protection experiments, 200 μg of poly(I:C) (Calbiochem) in phosphate-buffered saline was administered intracerebrally, and poliovirus challenge ($10^4$ PFU) was performed with the same inoculation routes on the next day.

**Determination of virus titer in mouse tissues.** Six mice inoculated with poliovirus were sacrificed on day 3 p.i. They were anesthetized and blood was collected from the heart. After perfusion with 20 ml of phosphate-buffered saline, the tissues were removed and frozen at −80°C. The tissues were thawed and homogenized in 5 to 10 ml of minimal essential medium. After centrifugation for 20 min at 3,000 × *g*, the virus titer of the supernatant was determined.

**Histological and immunological examinations.** Three to six mice were sacrificed on day 1, 2, or 3 p.i. or when the mice showed paralysis and were then used for histological examination. The mice were anesthetized and perfused with 10 ml of phosphate-buffered saline followed by 10 ml of 4% paraformaldehyde in phosphate-buffered saline. The fixed tissues were embedded in paraffin, from which 3-μm-thick sections were prepared. The poliovirus antigen was detected with an immunoperoxidase method as described previously (21).

**Alanine aminotransferase and amylase activity.** To evaluate the extent of liver injury in the mice, the serum alanine aminotransferase (ALT) level was measured with the Transnase Nissui kit (Nissui Pharmaceutical Co. Ltd.). The serum amylase level in the mice was measured by the method of Henkel et al. (12) with the Cica Auto amylase kit (Kanto Chemical Co. Inc.).

**Quantitative real-time PCR.** Mice tissues were separated immediately after sacrifice and stored at −80°C. Total RNA was isolated from the tissue with the RNeasy mini RNA isolation kit (Qiagen, Valencia, Calif.) according to the supplier's instructions. After DNase I treatment, cDNA primed with a random hexamer was synthesized with the Taqman reverse transcription reagent (Applied Biosystems, Foster City, Calif.). The quantification of RNAs was performed with ABI Prism 7900HT. 18S rRNA was quantified by the SYBR Green method with 18S-rRNA-F (5′-GTA ACC CGT TGA ACC CCA TT-3′) and 18S-rRNA-R (5′-CCA TCC AAT CGG TAG TAG CG-3′) as primers. Poliovirus RNA was quantified by the Taqman method with PV c-2493F (5′-TGG TTG GTG ACA GTT CTT ACA CAT T-3′) and PV c-2629R (5′-CCA CTG TGG CAC ACA GTG ATG-3′) as primers and PV c-2579T (5′-FAM-CCA TGT CGA ACG CAA AGC GCC-TAMRA-3′) as the probe. The detection of IFN-β, 2′-5′ oligoadenylate synthetase (OAS)1a, OAS1g, OAS2, OAS3, OASL2, protein kinase R, RIG-I, and helicard mRNAs was performed with Assay-on-Demand PCR probes (Applied Biosystems). The amount of mRNA was determined by comparison with standard templates of cloned cDNAs of known copy number. The expression levels were then normalized to the level of 18S rRNA.

## RESULTS

**Increased susceptibility of PVR-transgenic/*Ifnar* knockout mice to poliovirus.** We previously produced transgenic mice expressing the human *PVR* gene (20, 21). *PVR* mRNA was detected in the brain, spinal cord, thymus, lungs, heart, stom-

TABLE 1. Susceptibility to poliovirus infection

| Inoculation route | Mouse strain[a] | No. of mice dead/no. inoculated at inoculum dose ($log_{10}$ PFU/mouse): | | | | | | | | | | $LD_{50}$ ($log_{10}$) |
|---|---|---|---|---|---|---|---|---|---|---|---|---|
| | | −1 | 0 | 1 | 2 | 3 | 4 | 5 | 6 | 7 | 8 | |
| Intracerebral | PVR-tg | 0/6 | 1/6 | 1/6 | 1/6 | 4/6 | 5/6 | 6/6 | | | | 2.5 |
| | PVR-tg/*Ifnar* KO | 0/6 | 1/6 | 3/6 | 6/6 | 6/6 | | | | | | 0.8 |
| Intravenous | PVR-tg | | | 0/6 | 1/6 | 1/6 | 4/6 | 3/6 | 6/6 | | | 5.0 |
| | PVR-tg/*Ifnar* KO | | 0/6 | 0/6 | 5/6 | 6/6 | | | | | | 1.7 |
| Intraperitoneal | PVR-tg | | | | | | 0/6 | 1/6 | 3/6 | 5/6 | 5/6 | >6.2 |
| | PVR-tg/*Ifnar* KO | | 0/6 | 3/6 | 5/6 | 6/6 | | | | | | 1.2 |

[a] tg, transgenic; KO, knockout.

ach, and muscle at high levels, in the spleen and kidneys at intermediate levels, and in the liver at low levels (data not shown). The PVR-transgenic mice were susceptible to poliovirus infection via the intracerebral, intraperitoneal, and intravenous routes. The infected mice developed a paralytic disease resembling human poliomyelitis. Unlike humans, however, PVR-transgenic mice were not highly susceptible to oral infection with poliovirus. We performed subsequent experiments with this transgenic mouse model.

Mice lacking the alpha/beta IFN response become highly susceptible to several virus infections (26). We compared the susceptibility of PVR-transgenic mice with that of PVR-transgenic/*Ifnar* knockout mice to poliovirus infection via intracerebral, intravenous, and intraperitoneal inoculations. The mice showed paralysis and died within 2 weeks p.i. in a dose-dependent manner following inoculation via all routes. This suggested that the mice died mainly due to poliovirus infection in the central nervous system irrespective of the inoculation route. The results and the $LD_{50}$ values are shown in Table 1. The PVR-transgenic/*Ifnar* knockout mice were more sensitive to fatal poliovirus infection than the PVR-transgenic mice by any infection route. The $LD_{50}$ value for PVR-transgenic/*Ifnar* knockout mice inoculated intracerebrally was 50-fold lower than that for PVR-transgenic mice. Notably, PVR-transgenic/*Ifnar* knockout mice became 3,000- and >20,000-fold more sensitive to poliovirus via intravenous and intraperitoneal inoculation, respectively. Furthermore, $10^6$ PFU of poliovirus inoculated orally caused paralysis in 50% of the PVR-transgenic/*Ifnar* knockout mice (data not shown). On the contrary, PVR-transgenic mice with the disrupted IFN-γ gene (42) did not exhibit a significant increase in susceptibility to poliovirus infection (data not shown). The results indicate that alpha/beta IFN strongly influences poliovirus pathogenesis.

**Distribution of poliovirus infection in PVR-transgenic/*Ifnar* knockout mice.** Increased susceptibility to poliovirus by peripheral infection routes suggested that the poliovirus replicated efficiently in nonneural tissues. We compared poliovirus titers in the various tissues of nontransgenic C57BL/6 mice, PVR-transgenic mice, and PVR-transgenic/*Ifnar* knockout mice intravenously inoculated with $2 \times 10^7$ PFU of poliovirus. After intravenous inoculation, poliovirus was immediately delivered to all tissues, including the central nervous system, independently of the presence of PVR (47). Most of the PVR-transgenic mice and PVR-transgenic/*Ifnar* knockout mice developed paralysis by day 3 or 4 p.i., while the nontransgenic mice did not.

Figure 1 shows the virus load of various tissues on day 3 p.i. The virus titers in the brain and spinal cord of PVR-transgenic mice were much higher than those recovered from the same tissues of nontransgenic mice. The virus titer in the pancreas of PVR-transgenic mice was also higher than that of nontransgenic mice but not as high as the titers in the neural tissues of transgenic mice. The viral load of most of the other tissues of PVR-transgenic mice was slightly higher than that recovered from nontransgenic mice. These results suggest that poliovirus replicated efficiently in the central nervous system and less efficiently in the pancreas and did not replicate or replicated to only a slight degree in other nonneural tissues of PVR-transgenic mice. On the contrary, in PVR-transgenic/*Ifnar* knockout mice, poliovirus titers in all of the tissues examined were very high (Fig. 1), suggesting that the virus can replicate in nonneural tissues if alpha/beta IFN signaling is disrupted.

**Poliovirus replication site in the visceral tissues of PVR-transgenic/*Ifnar* knockout mice.** We investigated the localiza-

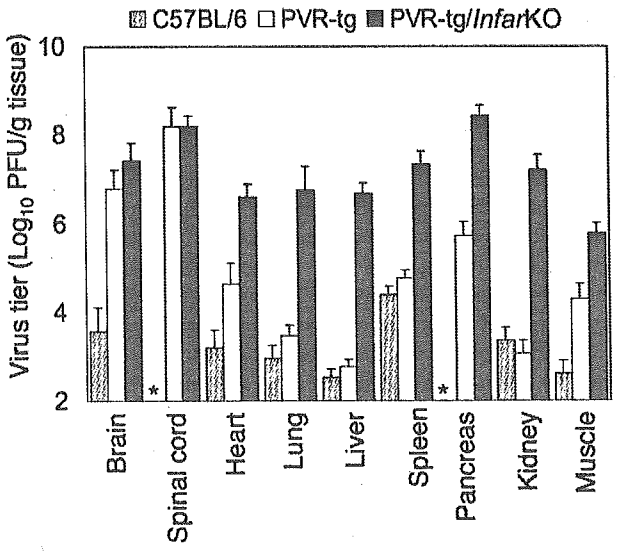


FIG. 1. Comparison of poliovirus titers in tissues of nontransgenic, PVR-transgenic, and PVR-transgenic/*Ifnar* knockout mice. The mice were inoculated intravenously with $2 \times 10^7$ PFU of poliovirus type 1 Mahoney strain. The tissues of nontransgenic mice (hatched bars), PVR-transgenic mice (open bars), and PVR-transgenic/*Ifnar* knockout mice (solid bars) were separated on day 3 p.i., and virus titers were determined by a plaque assay. The values represent the mean virus titer + standard deviation of six mice. The asterisk indicates that the values were below the limit of detection (2.0 $log_{10}$ PFU/g).

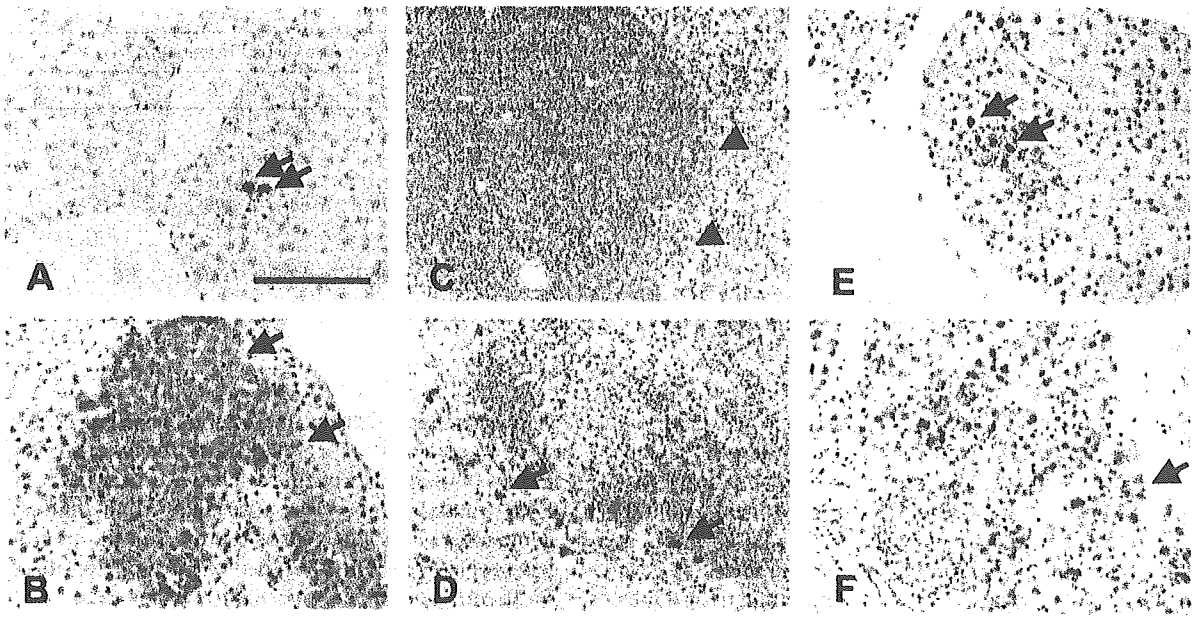


FIG. 2. Immunohistochemical detection of poliovirus antigen in infected mice. Poliovirus antigens were detected in PVR-transgenic (A, C, and E) and PVR-transgenic/*Ifnar* knockout (B, D, and E) mice with a rabbit polyclonal antibody recognizing the poliovirus capsid antigen. The mice were intravenously inoculated with $2 \times 10^7$ PFU of poliovirus. (A) Liver of the PVR-transgenic mice on day 1 p.i. Poliovirus antigen-positive cells, indicated by arrows, were focally observed with slight cellular infiltration around the infected cell. (B) Liver of PVR-transgenic/*Ifnar* knockout mice on day 1 p.i. Hepatic cells positive for poliovirus were observed in a zonal pattern. (C) Spleen of PVR-transgenic mice on day 1 p.i. A few very weakly stained cells are observed in the marginal zone, indicated by arrowheads. (D) Spleen of PVR-transgenic/*Ifnar* knockout mice on day 1 p.i. Many poliovirus antigen-positive large cells are localized in the marginal zone. The cells were identified as macrophages on the basis of the detection of CD11. (E) Pancreas of PVR-transgenic mice on day 3 p.i. A small cluster of cells positive for poliovirus antigen was observed in the lobulus in association with a slight inflammatory reaction. The poliovirus antigen was observed constantly in all mice. (F) Pancreas of PVR-transgenic/*Ifnar* knockout mice on day 3 p.i. Numerous acinar cells positive for the poliovirus antigen were distributed in many lobuli of the pancreas. Only a few poliovirus antigen-positive cells were observed in Langerhans' islets in the bottom left. (A) Bar, 125 μm.

tion of the poliovirus antigen and corresponding pathological changes to determine the virus replication sites. In the liver of PVR-transgenic mice, cells positive for the poliovirus antigen were detected occasionally, after careful observation. The antigens were found sporadically as a single cell or as a group of a few poliovirus antigen-positive cells with cellular damage in the liver on day 1 p.i., but were rarely detected after day 2 p.i. Inflammatory cell infiltration was also observed around the infected cells (Fig. 2A). Strong poliovirus antigen staining was not detected in the spleen, but a few very weakly stained cells were observed in the marginal zone (Fig. 2C). In the pancreas, groups of a few poliovirus antigen-positive cells were sporadically observed on day 1 p.i., with the number increasing slightly on day 3 p.i. (Fig. 2E). Although the infected area in the pancreas was not large, the antigens were always detected in all the mice. This observation is consistent with a higher poliovirus titer in the pancreas than in the other visceral tissues (Fig. 1).

In contrast, in PVR-transgenic/*Ifnar* knockout mice, zonal areas or clusters of poliovirus antigen-positive cells were observed in the liver on day 1 p.i. (Fig. 2B). These infected cells were identified morphologically as hepatocytes. The number of poliovirus antigen-positive cells decreased on day 3 p.i., but the inflammatory infiltrate became more evident. In the spleen, poliovirus antigen was detected mainly in large mononuclear cells in the marginal zone (Fig. 2D). These large mononuclear cells were positive for CD11 in serial sections and were shown to be macrophages (data not shown). In the pancreas, massive infection was observed in acinar cells (Fig. 2F).

The destruction of hepatocytes and pancreatic acinar cells was also confirmed by biochemical examination. Serum ALT and amylase levels were measured in intravenously inoculated mice on day 3 p.i. ALT values increased markedly in the PVR-transgenic/*Ifnar* knockout mice compared to the nontransgenic mice ($P < 0.05$, $t$ test), whereas there was only a slight increase in the PVR-transgenic mice (Fig. 3A). This result indicates destruction

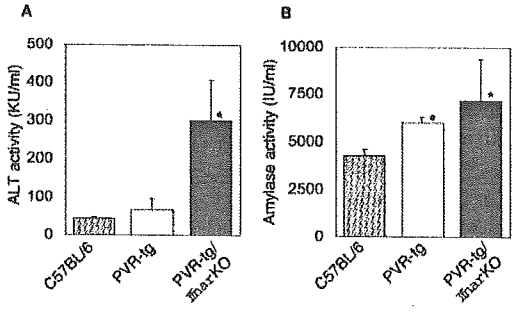


FIG. 3. Serum ALT and amylase activities in infected mice. The mice were inoculated intravenously with $2 \times 10^7$ PFU of poliovirus. The sera of nontransgenic (hatched bars), PVR-transgenic (open bars), and PVR-transgenic/*Ifnar* knockout (solid bars) mice were collected on day 3 p.i., and their ALT activity (A) and amylase activity (B) were determined. The mean values plus standard deviation of four mice are shown. The asterisks indicate that the values are significantly higher than those observed in the nontransgenic C57BL/6 mice ($P < 0.05$, $t$ test).

of hepatocytes in the PVR-transgenic/*Ifnar* knockout mice. The amylase activity values in the serum of PVR-transgenic mice were 1.3- to 1.5-fold (mean, 1.4-fold) higher than that of the nontransgenic mice ($P < 0.05$, $t$ test), while those of PVR-transgenic/*Ifnar* knockout mice were 1.2- to 2.3-fold higher (mean, 1.7-fold) than that of nontransgenic mice ($P < 0.05$, $t$ test) (Fig. 3B). The results indicated acinar cell destruction in the pancreas and/or salivary glands in PVR-transgenic and PVR-transgenic/*Ifnar* knockout mice. These observations further indicate that the loss of alpha/beta IFN signaling apparently alters the tissue tropism. The hepatocytes, acinar cells, and macrophages in the spleen became potentially permissive for poliovirus infection, indicating that they express host factors required to support poliovirus replication.

With PVR-transgenic/*Ifnar* knockout mice, the virus antigens were not clearly detected in the kidneys, heart, and lungs of poliovirus-inoculated mice. Similar experiments were performed with another PVR-transgenic mouse strain, PVRtg25 (46). In this mouse strain, *PVR* mRNA expression levels are higher than those of PVRtg21. We further crossed this strain with *Ifnar* knockout mice and examined the susceptibility of PVRtg25/*Ifnar* knockout mice to poliovirus. All of the inoculated mice became moribund with jaundice on day 1 p.i. Immunohistological examination revealed that viral antigen-positive cells were detected in the liver, spleen, pancreas, kidneys, and heart (data not shown). Poliovirus infection in the liver was associated with massive necrosis of the parenchymal cells, which was correlated with liver failure. This confirmed that poliovirus can also replicate in the kidneys and heart when IFN signaling is disrupted.

**Role of IFN in poliovirus spreading in the body.** The above data indicate that the IFN response is particularly effective in restricting virus replication in the visceral tissues. Viremia occurred as a consequence of virus multiplication in extraneural sites. It is possible that the IFN response influences virus titer and, accordingly, that IFN also contributes in decreasing the incidence of paralytic and fatal poliovirus infection by lowering the chance of poliovirus entry into the central nervous system. To demonstrate this, we compared the virus titers in PVR-transgenic and PVR-transgenic/*Ifnar* knockout mice. We determined virus titers in the plasma of PVR-transgenic and PVR-transgenic/*Ifnar* knockout mice infected intraperitoneally with poliovirus ($10^3$ PFU). This dose was employed because it is below the $LD_{50}$ of the PVR-transgenic and above that of the PVR-transgenic/*Ifnar* knockout mice (see Table 1).

Expectedly, a very high titer ($10^8$ to $10^9$ PFU/ml) of poliovirus was detected on day 3 p.i. in the PVR-transgenic/*Ifnar* knockout mice, resulting in the death of the mice at day 4 p.i. In contrast, less than $10^3$ PFU of poliovirus/ml was detected in the PVR-transgenic mice between days 2 and 5 p.i., and it was no longer detected at day 7 p.i. (Fig. 4). These results suggest that some cells, if not all, that express PVR can act as reservoirs of poliovirus during the progression of the disease in the viremic phase. However, only a small proportion of these cells produce poliovirus with a low efficiency because of the inhibitory effect of IFN, and high-titer viremia is prevented in animals with a normal IFN system. We consider that virus replication sites during the viremic phase have not been histologically identified because poliovirus replication levels are normally low in these cells in PVR-transgenic mice, monkeys, and humans.

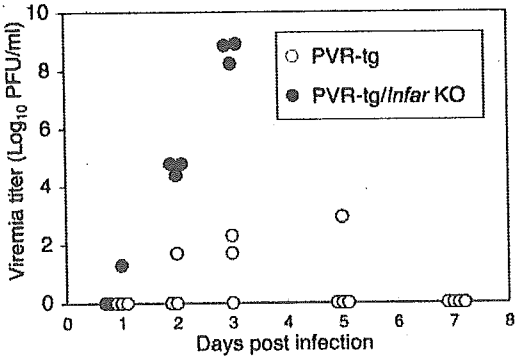


FIG. 4. Viremia in PVR-transgenic mice and PVR-transgenic/*Ifnar* knockout mice. Poliovirus ($10^3$ PFU) was inoculated intraperitoneally. Plasma from three or four infected mice was collected at the indicated day p.i., after which the virus titer in the plasma was determined. Open circles, PVR-transgenic mice; solid circles, PVR-transgenic/*Ifnar* knockout mice. Note that the virus titer in the PVR-transgenic/*Ifnar* knockout mice is very high. The data for PVR-transgenic/*Ifnar* knockout mice on days 5 and 7 p.i. were not available because all mice died on the fourth day after inoculation.

**Expression of IFN-β and ISGs in the host.** The susceptibility to poliovirus varied among the tissues. We therefore determined if the expression profiles of genes that confer an antiviral state in the IFN response were different between target and nontarget tissues. We determined the expression of mRNAs for IFN-β and ISGs with a quantitative real-time reverse transcription-PCR technique (Fig. 5). Since IFN-β is the first alpha/beta IFN induced after virus infection (36, 39, 41) and picornaviruses are known to be sensitive to OAS (7, 8) and protein kinase R (25), we focused on expression of IFN-β, OAS, and protein kinase R mRNAs. Of the ten genes that are similar to human OAS in the mouse genome, OAS1a, OAS1g, OAS2, OAS3, and OASL2 were shown to synthesize 2′-5′oligoadenylate (16).

We first determined the expression levels of IFN-β, OAS, and protein kinase R mRNAs in the noninfected PVR-transgenic mice. Very little expression of IFN-β mRNA was observed in all tissues of the noninfected mice (Fig. 5A). The expression levels of the mRNAs for OAS1a, OAS1g, OAS2, OAS3, OASL2, and protein kinase R are shown in Fig. 5B to G (open bars). The expression level of each ISG mRNA and the tissue distribution profiles were different. However, in general, they were expressed in the nontarget tissues more abundantly than in the target tissues of noninfected PVR-transgenic mice. No ISG was expressed at high levels in the central nervous system, an observation consistent with previous reports (1, 22, 30).

We then determined the changes in the expression levels of IFN-β and ISG mRNAs in the infected mice (Fig. 5A to G). On day 1 p.i., IFN-β mRNA expression in the spleen was observed at very high levels. Low-level IFN-β expression was observed in the heart, lungs, liver, kidneys, and muscle. No significant increase of IFN-β mRNA was observed in the brain and spinal cord on day 1 p.i. (Fig. 5A, gray solid bars). On day 3 p.i., IFN-β mRNA levels in the heart, lungs, liver, kidneys, and muscle decreased to nearly basal levels. In contrast, they increased to very high levels in the brain and spinal cord (Fig. 5A, solid black bars). Thus, the IFN-β mRNA expression pro-

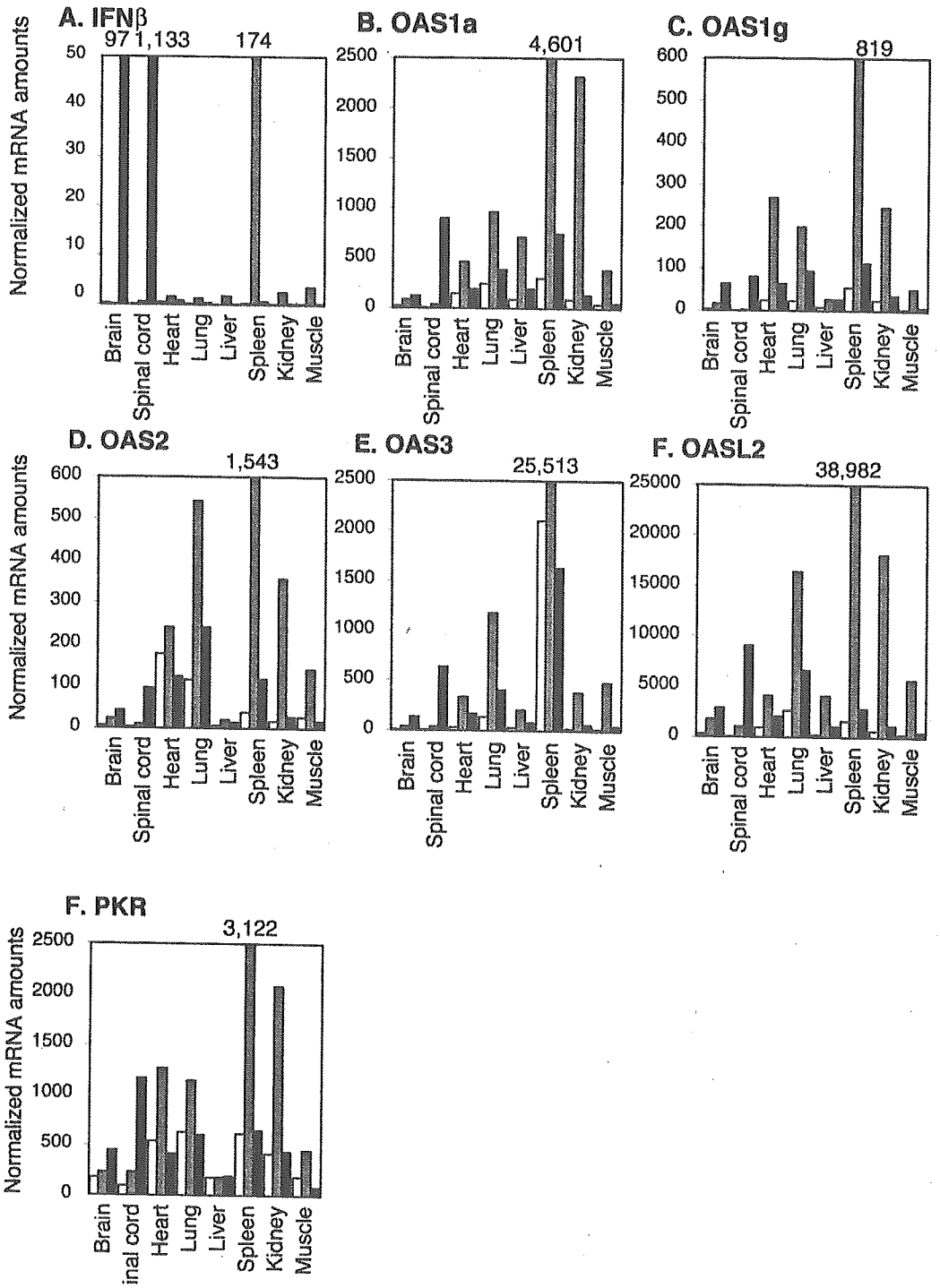


FIG. 5. Expression of IFN-β and ISGs in PVR-transgenic mice. The expression levels of IFN-β and ISG mRNAs in noninfected PVR-transgenic mice and PVR-transgenic mice infected intravenously with poliovirus ($2 \times 10^7$ PFU) were determined by real-time quantitative PCR. The amounts of IFN-β (A), OAS1a (B), OAS1g (C), OAS2 (D), OAS3 (E), OASL2 (F), and protein kinase R (G) mRNAs normalized to $10^7$ copies of 18S rRNA are shown. Open bars, gray solid bars, and black solid bars indicate the results for noninfected mice, infected mice at 1 day p.i., and infected mice at 3 days p.i., respectively. The mean values for three to six mice are indicated. The numbers above each figure indicate values that could not be represented within the figures. Note that the open bars in A are not visible because IFN-β mRNA expression in the noninfected mice was very low.

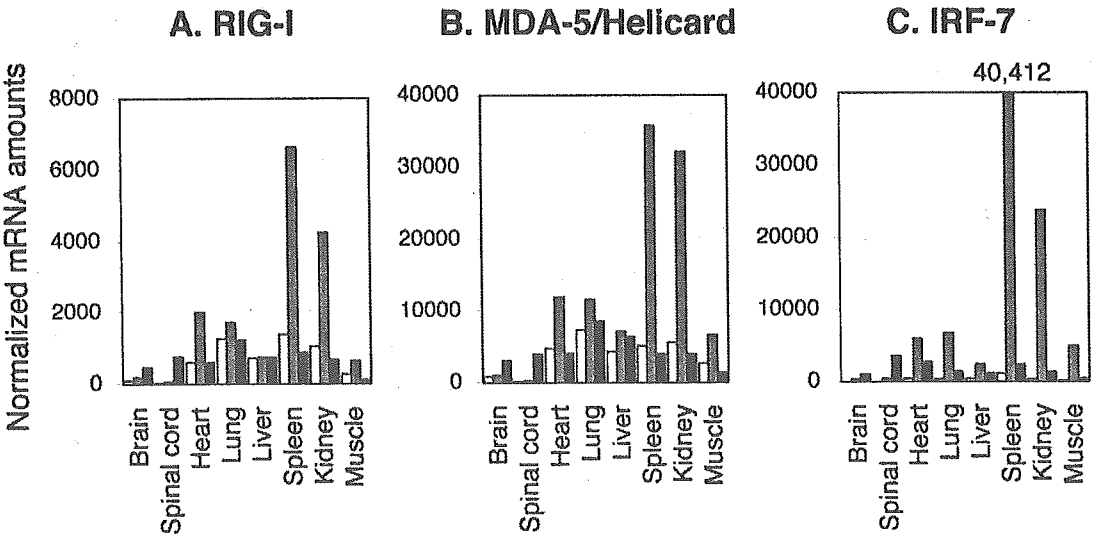


FIG. 6. Expression of RIG-I, helicard, and IRF-7 mRNAs in PVR-transgenic mice. The expression levels of RIG-I, helicard, and IRF-7 mRNAs of noninfected PVR-transgenic mice and PVR-transgenic mice infected intravenously with poliovirus ($2 \times 10^7$ PFU) were determined by real-time quantitative PCR. The mean values for three mice are indicated. The amounts of RIG-I (A), helicard (B), and IRF-7 (C) mRNAs were determined. Open bars, gray solid bars, and black solid bars indicate the results of noninfected mice, infected mice at 1 day p.i., and infected mice at 3 days p.i., respectively. The amounts of mRNA per $10^7$ copies of 18S rRNA are shown.

files are different between target tissues and nontarget tissues in poliovirus-infected mice.

The expression levels of ISG mRNAs also changed after poliovirus infection, consistent with the change in IFN-β mRNA levels (Fig. 5B to G, gray and solid black bars). The ISG expression pattern was clearly different between the target and nontarget tissues. ISG mRNAs increased in most of the visceral tissues on day 1 p.i. The expression level of ISG mRNAs increased most efficiently in the spleen. The levels of ISG mRNAs were relatively high in the heart, lungs, liver, kidneys, and skeletal muscle. In these tissues, the viral load was low (Fig. 1), and the poliovirus antigen was not detected. This indicates that ISG induction in these tissues was sufficient to inhibit poliovirus replication. The expression levels of ISG mRNAs in these tissues decreased on day 3 p.i., with a corresponding decrease in IFN-β mRNA levels. In the brain and spinal cord, however, significant induction of ISG mRNAs was not observed on day 1 p.i. The induction became evident only on day 3 p.i., when poliovirus destroyed a large number of neurons. We also noticed that the ratio of ISG and IFN-β mRNAs (ISG/IFN-β mRNA) in the brain and spinal cord on day 3 p.i. was much lower than that in nontarget tissues on day 1 p.i. (Fig. 5A to G). This indicates that the IFN response did occur in neurons in the brain and spinal cord but was not sufficient and failed to inhibit viral growth in the early phase of infection.

**Expression of RIG-I, MDA-5/helicard, and IRF-7 in target and nontarget tissues.** The data suggests that neurons in the target tissues failed to respond sufficiently to poliovirus infection. It is possible that there is a difference in the expression mechanism of the IFN response. We proceeded to examine a regulatory factor required for IFN response. Yoneyama et al. recently found that RIG-I functioned as a detector of intracellular double-stranded RNA. The cells that express this gene at high levels in vitro can induce IFN in an accelerated fashion and can survive against encephalomyocarditis virus and vesicular stomatitis virus infection (48). MDA-5/helicard is another caspase recruitment domain (CARD)-containing helicase, which is implicated as having a function similar to that of RIG-I (48). Both RIG-I and MDA-5/helicard are inducible by IFNs (17, 48).

Figures 6A and B show the changes in the RIG-I and MDA-5/helicard levels, respectively. Like that of other ISGs, the expression of these genes is low in the brain and spinal cord but high in nontarget tissues in the noninfected mice. The response of these genes after poliovirus infection is similar to that of other ISGs. They were induced at high levels in the nontarget tissues on day 1 p.i. but not in the target tissues. Thus, the nontarget tissues that expressed RIG-I and MDA-5/helicard at high levels may have an advantage in inducing IFN-β soon after poliovirus infection. We also examined the expression of IRF-7, another regulatory factor involved in the activation of IFN-α genes. IRF-7 thus is important to amplify the IFN response (37). The expression profile of IRF-7 was also similar to those of other ISGs (Fig. 6C).

**Protection of mice from poliovirus infection by poly(I:C) treatment.** The preceding data suggest that neurons in the brain and spinal cord were highly susceptible to poliovirus because expression levels of ISGs, including OASs and RIG-I, were low in the noninfected state. If this is the case, pretreatment to induce the antiviral state in the central nervous system would increase the survival rate of poliovirus-infected mice. Hence, treatment with poly(I:C) is expected to induce IFNs and ISGs and establish an antiviral state.

Poly(I:C) (200 μg) was administered intracerebrally to PVR-transgenic mice, and on the next day, RNA was prepared from the brain and spinal cord. The levels of OAS1a and RIG-I were determined by real-time quantitative PCR. As expected, expression of the mRNAs for OAS1a and RIG-I was elevated to high levels by poly(I:C) (Fig. 7A and B). PVR-transgenic mice treated with poly(I:C) or mock treated were challenged with poliovirus